



Geostatistical Seismic Inversion of the Arruda Sub-Basin, Portugal

Ana Carolina Mateus Moreira

Thesis to obtain the Master of Science Degree in

Petroleum Engineering

Supervisor: Dr. Leonardo Azevedo Guerra Raposo Pereira

Examination Committee

Chairperson: Prof. Maria João Pereira

Supervisor: Dr. Leonardo Azevedo Guerra Raposo Pereira

Members of the Committee:

Eng. Dario Sergio Cersósimo

October 2015

This page was intentionally left blank

“Started from the bottom, now we’re here.”

D.

This page was intentionally left blank

Acknowledgments

The following work would not have been possible without the data available from the Divisão de Pesquisa e Exploração de Petróleo (DPEP), now ENMC (UPEP-Unidade de Pesquisa e Exploração de Recursos Petrolíferos).

I would like to thank to Dr. Leonardo Azevedo, my advisor, for all the support and words of encouragement, during this 2 years of the Master's.

Abstract

With the increasing complexity of hydrocarbons reservoirs there is a constant need of combining different kinds of information, such as geological (e.g. basin characterization, main petroleum systems, structural and geodynamic history, stratigraphical units and main paleoenvironments), *seismic reflection data* (e.g. seismic interpretation and seismic inversion), *well logging*, (e.g. petrophysical properties and formation evaluation) and *geostatistical modeling* to characterize the spatial distribution of the subsurface properties of interest in order to provide the best insight for an unexplored area.

This thesis consists on the evaluation of a portion of the Arruda sub-basin from the Lusitanian Basin, Portugal, with the integrated interpretation of: geological data, seismic interpretation of two 2D seismic lines, interpretation of the well logs from the well Benfeito-1, and finally the inference of the subsurface elastic properties recurring to a geostatistical seismic inversion.

This work aims to provide an exploration assessment for the regional geology in the Arruda Sub-basin from the Lusitanian Basin, Portugal, for its hydrocarbon potential. This goal is achieved with a new re-interpretation of the available 2D seismic reflection section and well-log data and, for the first time, the inference of subsurface elastic properties recurring to geostatistical seismic inversion.

One of the novel approaches of this work is the way geostatistical seismic inversion was used in an unexplored area with no well-log data to assess its potential in hydrocarbons. This is a different type of work from the ones published using geostatistical seismic methodologies, that are generally used for a large scale information 3D seismic cube, with well-log data from at least a few number of wells.

Keywords: Geostatistical Seismic Inversion for undersampled basins, Hydrocarbon Exploration, Arruda Sub-basin, Seismic Interpretation, Well-logging Evaluation.

Resumo

Com o aumento da complexidade dos reservatórios de hidrocarbonetos, existe uma constante necessidade de combinar diferentes tipos de informação do tipo: geológico (caracterização da bacia sedimentar, dos sistemas petrolíferos, caracterização da estrutura e da história geodinâmica e da definição de paleo-ambientes), sísmica de reflexão (interpretação sísmica e inversão sísmica), diagrfias (propriedades petrofísicas e avaliação de formações) e modelação geostatística para caracterizar a distribuição espacial de propriedades da sub-superfície de interesse, de forma a fornecer uma melhor avaliação.

Esta tese consiste na avaliação de uma parte da Bacia da Arruda, que pertence à Bacia Lusitânica em Portugal, com a integração da interpretação de diferentes tipos de informação: geológica, sísmica (com a interpretação de duas linhas sísmicas em 2D), interpolação de diagrfias do poço Benfeito-1 e finalmente a aferência de propriedades elásticas da sub-superfície recorrendo ao algoritmo de inversão geostatística.

Este trabalho providencia uma avaliação exploratória, para a geologia regional da Sub-Bacia da Arruda da Bacia Lusitânica, Portugal para o potencial de hidrocarbonetos.

Relativamente ao seu contributo este procura providenciar mais informação da Sub-bacia da Arruda com uma reinterpretação da informação de sísmica de reflexão disponível, e das diagrfias com a inferência em propriedades elásticas da sub-superfície recorrendo ao algoritmo de inversão geostatística.

O seu objectivo é uma re-interpretção dos dados disponíveis em 2D de sísmica de reflexão com os dados de diagrfias e com a inferência primordial de propriedades elásticas da sub-superfície recorrendo ao método de inversão sísmica geostatística.

A nova abordagem deste trabalho é a forma como a inversão sísmica geostatística é aplicada em áreas pouco exploradas com pouca informação de diagrfias para determinar o potencial em hidrocarbonetos. Este é um trabalho diferente de todos os já publicados usando os métodos de geostatística, que geralmente são usados para informação em grande escala, como cubos de sísmica 3D, com informação de diagrfias de poço.

Palavras-Chave: Inversão Sísmica geostatística para áreas pouco exploradas, Exploração de Hidrocarbonetos, Sub-Bacia da Arruda, Interpretação Sísmica, Avaliação de Diagrfias e Petrofísica.

This page was intentionally left blank

Table of Contents

1. Introduction	13
1.1 Relevance of the Study.....	15
1.2 Aims and Objectives.....	15
1.3 Structure of the thesis	15
2. Geological Framework of the Arruda Sub-basin (<i>Lusitanian Basin, Portugal</i>).....	17
3. Petrophysics	25
4. Seismic Data	28
4.1 Seismic Reflection Method.....	28
4.2 Seismic Interpretation	31
4.3 Seismic Inversion.....	33
5. Case Study	35
5.1 Data-set.....	35
5.2 Petrophysical Analysis	37
5.3 Seismic Interpretation	42
5.4 Seismic Inversion.....	52
5.5 Integration of the Interpretation	65
6. Conclusion	66
7. References	67

List of Figures

Figure 1 - Contracts for exploration active in Portugal, including the Lusitanian Basin, at 2015 (adapted from DPEP 2015)	14
Figure 2 - The position of the Lusitanian Basin in Portugal today with its boundaries and offshore extension included. And the Central Lusitanian Basin where the study area is with detail, faults, diapiric structures, seismic lines and Benfeito-1 well from the data set. Adapted from Alves et al. (2003).	19
Figure 3 - Models for the deposition and geodynamics of the 3 sub-basin of the Lusitanian Basin the geological legend of the units is the same in both figure 3 a) and b). Adapted from the MILUPOBAS, 1995 report – Lornholt et al, 1995	20
Figure 4 - Summary of the Mesozoic lithostratigraphy of the southern part of the Lusitanian Basin, and seismic horizons interpreted (<i>Adapted from Alves et al, 2003.</i>).....	21
Figure 5 - The Mesozoic Petroleum System chart adapted for the age of the units in the study area. <i>Adapted from Pena & Pimentel, 2014.</i>	24
Figure 6 – Basic processing sequence for seismic data, adapted from Azevedo (2013).	30
Figure 7 - Shot Gather for an onshore acquisition.	30
Figure 8 - The tree types of reflectors stratification configuration, first for simple, second for progradational and third for complex.....	32
Figure 9 - Schematic representation of the Geostatistical Seismic Inversion; Adapted from Azevedo, (2013)	34
Figure 10 - Study area, including 3 Geological Maps of Portugal, of 3 areas: 30-B – Bombarral, 30-D Alenquer and 34-B Loures, note the Maps were cropped into exclusively the study area of the data set.	35
Figure 11 - Location of the (AR09_80-MIG and AR05_80-MIG) seismic lines plus the location of the Benfeito Well	36
Figure 12 - Example of the well logs presented on the Benfeito-1 well.	37
Figure 13 - Benfeito-1 Well Tops, and “reservoir” areas has “stars” on the report.	37
Figure 14 - Summary of the values obtain for different petrophysical parameters for the main units...	38
Figure 15 - Sonic-log derived Porosity (Wyllie <i>et al.</i> , 1958) for Montejunto Formation.....	39
Figure 16 - Sonic-log derived Porosity (Wyllie <i>et al.</i> , 1958) for Brenha Formation (Callovian).....	39
Figure 17 - Sonic-log derived Porosity (Wyllie <i>et al.</i> , 1958) for Candeeiros Formation	40

Figure 18 - Sonic-log derived Porosity (Wyllie <i>et al.</i> , 1958) for Brenha Formation (Aalenian-Pliensbachian)	40
Figure 19 - Sonic-log derived Porosity (Wyllie <i>et al.</i> , 1958) for Coimbra Formation.	41
Figure 20 - AR05_80-MIG Seismic Line.....	42
Figure 21 - AR05_80-MIG Seismic Line interpreted.	43
Figure 22 - AR09_80-MIG Seismic Line.....	43
Figure 23 - AR09_80-MIG Seismic Line interpreted.	44
Figure 24 - Interpretation of AR09_80-MIG Seismic Line, from the MILUPOBAS report.	45
Figure 25 - Projection of the Benfeito-1 Well, Frexial-1 Well and Arruda-1 Well, showing the huge variation in thickness for the Abadia Formation on the southern part of the Seismic Line AR09_80-MIG.	46
Figure 26 - Interpretation from Leinfelder and Wilson, showing Arruda-1 well drilled above an antithetical fault, related to the Arruda sub-basin boundary fault	47
Figure 27 – Summary of the main horizons interpreted and the analyses based on internal configuration, continuity and amplitude strength, for the AR09_80-MIG and AR05_80-MIG Seismic lines.....	48
Figure 28 - Isopachs for Abadia Fm, Montejunto Fm, Cabaços Fm, Brenha Fm and Dagorda Fm, respectively.....	51
Figure 29 –Result form (1-1) case for the GSI for AR05_80-MIG seismic line.	52
Figure 30 - Result form (3-17) case for the GSI for AR05_80-MIG seismic line.....	53
Figure 31 - Result form (6-32) case for the GSI for AR05_80-MIG seismic line.....	53
Figure 32 - Result form (1-1) case for the GSI for AR09_80-MIG seismic line.....	54
Figure 33 - Result form (3-17) case for the GSI for AR09_80-MIG seismic line.....	54
Figure 34 - Result form (6-32) case for the GSI for AR09_80-MIG seismic line.....	55
Figure 35 - The first image, is the real AR05_80-MIG Seismic line and the horizons marked. The second image is the zones for each of the horizons marked. Note the two images had the seismic already cropped to interest area.....	56
Figure 36 - The first image, is the real AR09_80-MIG Seismic Line and the horizons marked. The second image is the zones for each of the horizons marked. Note the two images had the seismic already cropped to interest area.....	57

Figure 37 - Log data from the Benfeito well. Track 1 the RHOB log; track 2 the Velocity log; track 3 the AI calculated from track 1 and 2; track 4 the AI resulting from the derivation of the Gardner's equation and last track 5 the RHOB obtain with the Gardner's equation.....	58
Figure 38 - Result form (1-1) case for the GSI with zones for AR05_80-MIG seismic line.....	59
Figure 39 - Result form (3-17) case for the GSI with zones for AR05_80-MIG seismic line.....	59
Figure 40 - Result form (6-32) case for the GSI with zones for AR05_80-MIG seismic line.....	60
Figure 41 - Correlation Coefficient Values for the corresponding 3 images on figure 38, 39 and 40. ..	60
Figure 42 - Result form (1-1) case for the GSI with zones for AR09_80-MIG seismic line.....	61
Figure 43 - Result form (3-17) case for the GSI with zones for AR09_80-MIG seismic line.....	61
Figure 44 - Result form (6-32) case for the GSI with zones for AR09_80-MIG seismic line.....	62
Figure 45 - Correlation Coefficient Values for the corresponding 3 images on figure 42, 43 and 44. ..	62
Figure 46 - Seismic lines AR05_80-MIG, real and synthetic seismic.	63
Figure 47 - Seismic lines AR05_80-MIG, real and synthetic seismic.	64

1. Introduction

Over the years the Oil and Gas industry has been in constant change passing through highs and lows producing from simple and huge onshore reservoirs to complex and very heterogeneous reservoirs from the deep offshore. Nowadays both exploration and production have become more complex and costly and in this way, there has been huge efforts to improve the subsurface characterization of under-explored areas, or even to provide the best subsurface inference during production phases, minimizing the costs is highly used and increasing the profit.

In early exploration cases with few data available, frequently with only seismic reflection and well-log data, geostatistical methodologies have proven to be a good solution to infer the subsurface properties of interest, both elastic and petrophysical while assessing the intrinsic spatial uncertainty of these properties.

In Portugal, the Lusitanian Basin is an example of a promising sedimentary basin, well known for its petroleum exploration potential, where however there is a low density of exploratory wells only; 2,4 wells for 1000 km².

The exploratory evaluation of the Lusitanian basin has been very encouraging over the years and there's no doubt about the presence of hydrocarbons. Studies performed in the 70's have proven the presence of all the "magic five" (source rock, overburden rock, seal, trap and migration) components needed to produce hydrocarbons; however, there's no proven economical accumulation of hydrocarbons in Portugal, according to several studies provided during the time. Proof of this potential is the continuous investment from different companies in new blocks, both offshore and onshore, in order to find potential hydrocarbon accumulations with a commercial value.

During 1938 and 1968, when the license for oil exploration in the Lusitanian Basin and Algarve Basin was accepted, these international oil and gas companies acquired mono-channel seismic reflection data, gravimetric data and they drill 78 shallow exploratory wells, only 33 with more than 500m of depth, according to the Divisão de Pesquisa e Exploração de Petróleo in Portugal (DPEP).

After these licenses, and with new legislation for oil exploration, the Portuguese basins were divided in blocks, both offshore and onshore, and resulting on more information and studies with the acquisition of about 21237 linear km of seismic surveys and 22 wells, and even drillstem test in 2 wells. More recently in 2007, 3 contracts were awarded to the consortium of (Hardman/Galp/Partex), in the deep-offshore of the Alentejo Basin, 4 contracts with (Petrobras/Galp/Partex) in the deep-offshore of the Peniche Basin, and finally 5 contracts with the company Mohave Oil and Gas Corporation for the onshore and offshore of The Lusitanian Basin, (Figure 1,).

In 1995 the MILUPOBAS project (*Multidisciplinary investigation leading to advanced knowledge of the Lusitanian and Porto basins of Portugal and their hydrocarbon potential*), developed a report called

Seismic Interpretation and Mapping of the Lusitanian Basin, Portugal, which fulfill regional seismic evaluation, seismic stratigraphy and depth conversion of selected areas in the Lusitanian and Porto basins, Portugal. It was originally signed by the Geological Survey of Denmark (GSD), which in the meantime was merged with the Geological Survey of Greenland under the new name: Geological Survey of Denmark and Greenland (GEUS). The newly merged institution has continued the responsibilities within the project as originally agreed in the contract.

The Gabinete para a Pesquisa e Exploração de Petróleo (GPEP), who acted as project coordinator, supplied all the data; copies of about 9700 km in seismic data and well data including logs, reports, and velocity information from some 40 wells. In terms of the data available for this thesis, GPEP provided the seismic lines, the well-logs, the Well Report and the *Seismic Interpretation and Mapping of the Lusitanian Basin, Portugal, 1995 MILUPOBAS* report.

The location of the data according to the report is considered *L5a*, and it stretches from latitude 38° 30' N in the south to the northern part of the so called Bombarral Sub-basin north of the Peniche peninsula at 39° 28' N. Geologically the mapped area covers three sub-basins: The Arruda, the Turcifal and the Bombarral sub-basins.

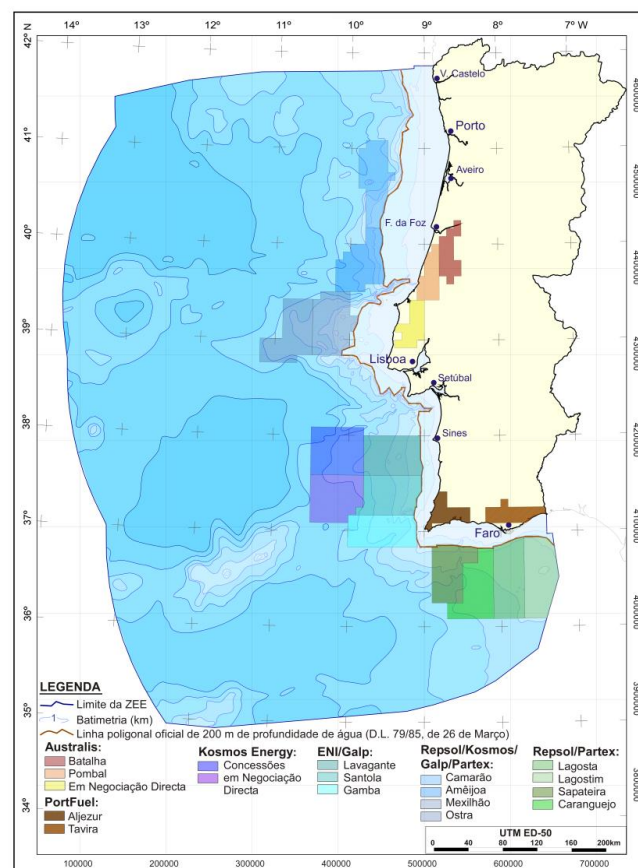


Figure 1 - Contracts for exploration active in Portugal, including the Lusitanian Basin, at 2015 (adapted from DPEP 2015)

1.1 Relevance of the Study

This study intends to contribute with a new understanding of the Arruda Sub-basin with a new re-interpretation of available seismic reflection and well-log and the inference of subsurface acoustic properties recurring to geostatistical seismic inversion.

It's also important to highlight that this work is a multi-disciplinary approach, a different type from the ones published so far for this study area, since it encompasses geostatistical seismic inversion for under-sampled basin with well-log data interpretation and seismic interpretation.

1.2 Aims and Objectives

This thesis consists on the evaluation of a portion of the Arruda sub-basin, Portugal from the integrated interpretation of geological data, seismic interpretation of two 2D seismic lines, the interpretation of the well logs from the well Benfeito-1, and finally the inference of the subsurface elastic properties recurring to a geostatistical seismic inversion algorithm.

This work aims to provide an exploration assessment for the regional geology in the Arruda Sub-basin from the Lusitanian Basin, Portugal, in terms of its hydrocarbon potential.

1.3 Structure of the thesis

This thesis is organized in seven chapters; the first chapter is the introduction of the work including the relevance of the study, and the main aims and objectives, presenting a scope of the work.

The chapter two is about a geological framework of the study area Arruda Sub-basin, from the Lusitanian Basin, Portugal. It includes a brief description of the geographic, geological, geodynamic characteristics, and description of the main lithostratigraphic units, presented in the Arruda Sub-Basin, with importance on the hydrocarbon exploration.

Chapter three presents an introduction to the well logging and the application of some equations in order to obtain petrophysical parameters

On chapter four, is all about seismic reflection method, with a brief description on the acquisition method, the interpretation and the seismic inversion technique used under the scope of this work.

Chapter five presents the case study the re-interpretation of two 2D seismic lines (AR09_80-MIG and AR05_80-MIG) in comparison with some interpretations done by authors in the past the petrophysical analysis of the available well and the results of the geostatistical seismic inversion.

Finally, chapter six summarizes the main conclusions and provides insights for new studies within the basin.

2. Geological Framework of the Arruda Sub-basin (*Lusitanian Basin, Portugal*)

The Lusitanian Basin, is a Mesozoic Atlantic Margin basin (peri-atlantic basin), located along the western Iberian margin, in the west-central part of the Portuguese mainland, covering about 22000 km².

The formation of this sedimentary basin is related with the opening of the North Atlantic Ocean during the Cretaceous and filled with approximately, 5 km of sediments from the Upper Triassic to the Cretaceous, covered with Cenozoic sediments. Structurally this basin limited by Porto-Tomar fault to the East, the granitic and metamorphic Berlengas horst to the West, the Porto Basin to the NW and the Arrábida Fault to the South, (Figure 2).

The evolution of the Lusitanian Basin be divided into 4 main geodynamic steps which comprises four unconformity bounded sequences according to (Wilson, 1988):

1. *Triassic-Callovian* – This sequence is typical of the early rift-sag successions encountered in most North Atlantic margin basins, (Ellis et al, 1990).

The basin infill took place in grabens and half-grabens, the Triassic red fluvial siliclastic materials (Silves Formation) were capped by the Hettangian evaporites (Dagorda Formation). These evaporites influenced the manner of the reactivation of the Hercynian basement faults, affected the cover of younger sediments. The deposition of the Coimbra, Brenha and Candeeiros formations occurred over a westerly dipping gentle slope. The carbonates are interbedded with shale, and locally turbidite beds occur. Some of the shales interbedding the Brenha Formation are rich in organic matter.

2. *Middle Oxfordian-Berriasian*. - The deposition took place over a basinwide hiatus, that may be related with the events from the opening of the southern North Atlantic, from the Late Callovian to the Lower Oxfordian. This is generally described as the rifting and thermal subsidence phase. This resulted in a widespread carbonate deposition (Cabaços formation).

This formation (Cabaços), contains highly bituminous horizons and is considered to be the major source for the many hydrocarbons shows in the southern part of the Lusitanian Basin, (Ellis et al, 1990). An eustatic equilibrium was achieved with the sedimentation of the shelf carbonates of the Montejunto Formation, which present strong facies and thickness variations (J.Carvalho et al.2005). After an abrupt rise in the relative sea-level accompanied by an uplift during the early Kimmeridgian ended the carbonate deposition, and this was followed by an influx of siliclastic materials, represented by the Abadia Formation.

3. *And 4 Valangian-Lower Aptian (Cretaceous). Upper Aptian-Turonian (Cretaceous)*. This two phases (3 and 4), considered as a single one for some authors, the sequences show a similar facies distribution, whit fluvial sands in the north being replaced southwards by marine marls and rudist

limestones. In the geodynamical point of view, they are associated with a rifting and an ocean spreading around North and Northwest of the Iberia.

Tectonically the Lusitanian Basin exhibits two distinct styles: one dominated by halokinetic structures and the other by faulting associated with the opening of the Atlantic Ocean. These structures show a dominant NNE-SSW orientation, plus a minor NE-SW trend, both of which mirror the trends of Hercynian basement faults (Wilson, 1988).

According to Kullberg et al. (2013), the Lusitanian basin can be divided in three distinct sectors based on facies variations thickness of lithostratigraphic units, and tectonic boundaries (Figure 2)

- Northern Sector (*NBL*), limited to the south by the fault of Nazaré, with a great thickness of sediments deposited during the Jurassic Lower - Middle and Upper Cretaceous.
- Central Sector (*CLB*), where the study area is located situated, between Nazaré's fault in the north, and Torres Vedras-Montejunto – Arrife on the south, where the Jurassic increases its thickness Eastwards, corresponds roughly to the recharge area of current Estremadura Limestone Massif (MCE – Maciço Calcário Estremenho).
- Southern Sector (*SLB*), bordered to the north by the failures Torres Vedras- Montejunto-Arrife and marked by the importance a high rate of sedimentation from the Upper Jurassic-Lower Cretaceous;

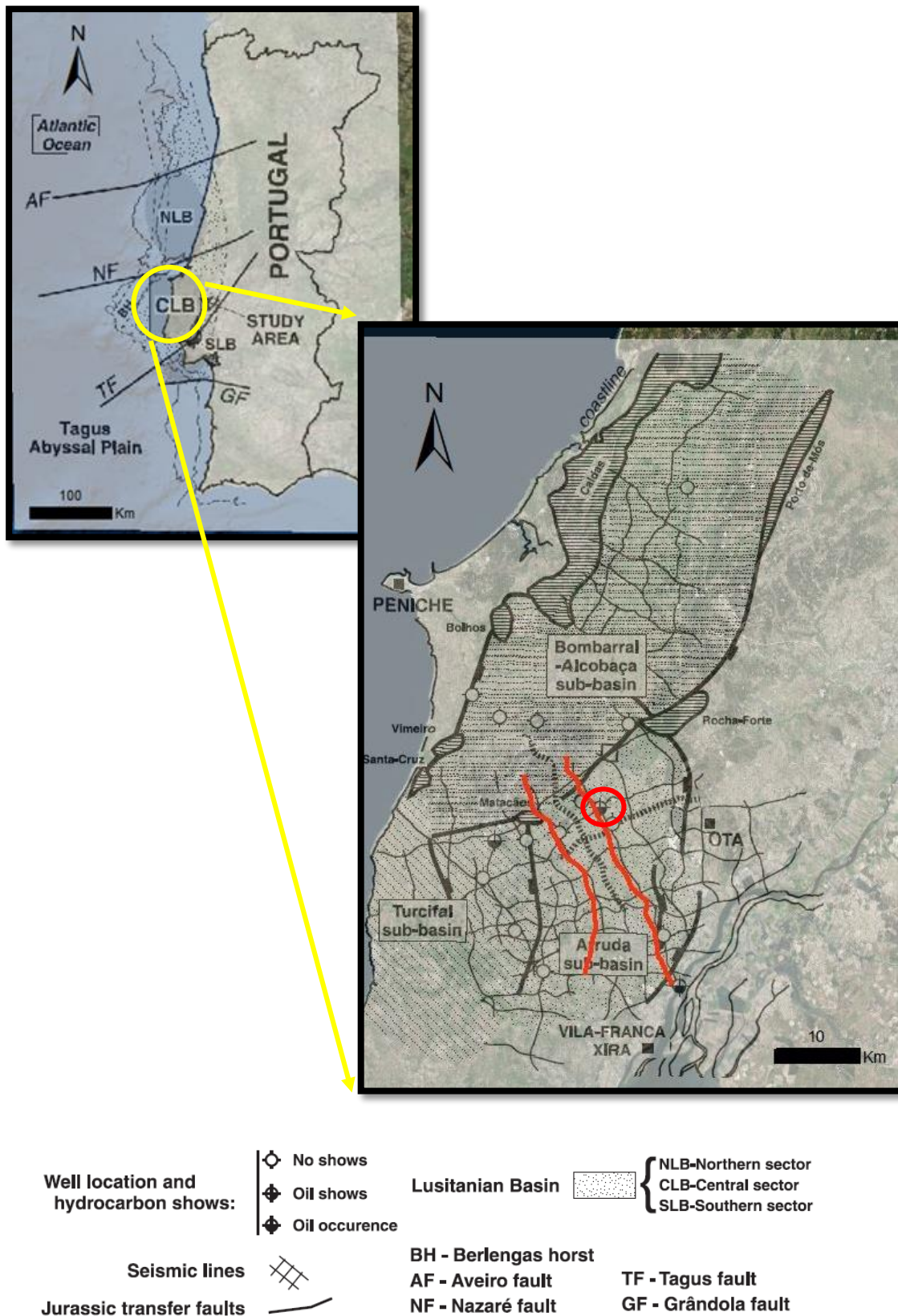


Figure 2 - The position of the Lusitanian Basin in Portugal today with its boundaries and offshore extension included. And the Central Lusitanian Basin where the study area is with detail, faults, diapiric structures, seismic lines and Benfeito-1 well from the data set. Adapted from Alves et al. (2003).

The Arruda sub-basin located on the *CLB* division of the Lusitanian Basin, corresponds to a half-graben developed during the Middle Oxfordian-Late Oxfordian as a consequence of transtensional rifting episodes that have affected the Estremadura Basin. This sub-basin represents an intra-continental pull-apart basin with a rhomb-like shape (Leinfelder & Wilson, 1989).

Turcifal and Arruda sub-basin are divided by an average of 20km long north to North-Northeast striking Runa Fault Complex; and Turcifal and Arruda half grabens are separated from Bombarral-Alcobaça sub-basin by 70km long northeast to east trending structural lineament; the Torres Vedras- Montejunto lineament, (Figure 2 and 3).

The development of complex fault- and diapir-bound sub-basins resulted by the presence of halite at depth (latest Triassic–Hettangian age, Dagorda Formation) limited and modified the propagation of basement faults into the post-salt overburden, contributing to the development of salt pillows and extensionally-forced folds during the Jurassic extensional phases (Alves et al., 2003) This development resulted in the separation the southern part into two half-grabens resulting in Arruda and Turcifal sub-basins with the consequent salt moving from the Arruda Sub-basin into the Montejunto Anticline separated the Arruda and Bombarral Sub-basins.

Figure 3 a) shows the schematic representation of the evolution between the Bombarral and Arruda sub-basin, which are divided by the Torres Vedras and Montejunto lineament. Figure 3 b) shows the evolution between Turcifal and Arruda sub-basin, disconnected by the Runa Complex. In both depositional models the Hettangian, Dagorda Formation movement, was critical to the reactivation of the Hercynian faults and deformation of the upper sediments.

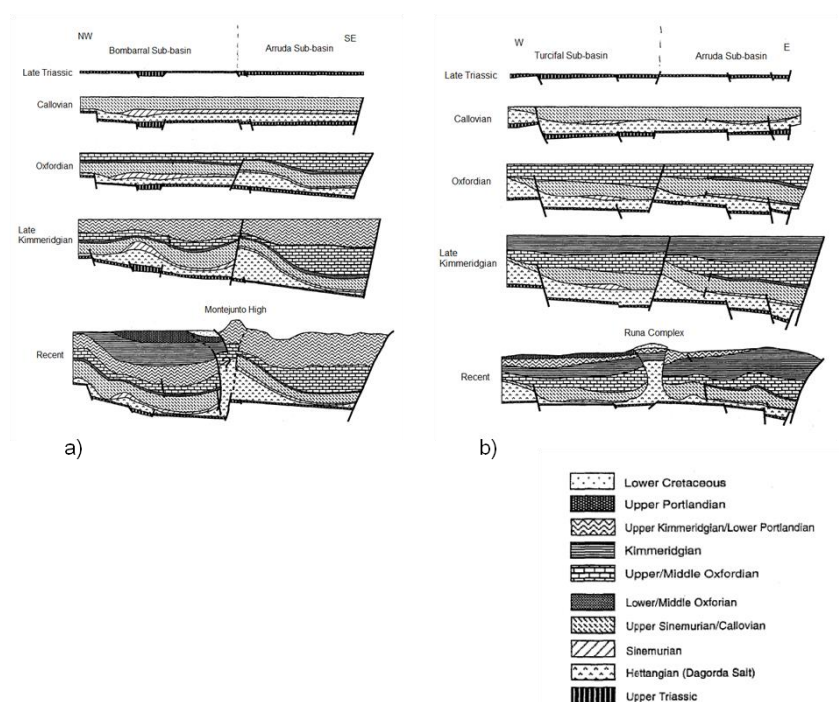
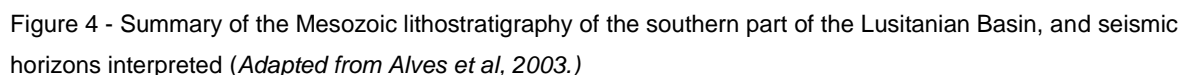


Figure 3 - Models for the deposition and geodynamics of the 3 sub-basin of the Lusitanian Basin the geological legend of the units is the same in both figure 3 a) and b). Adapted from the MILUPOBAS, 1995 report – Lornholt et al, 1995

Here we only describe the formations that were part of the well tops set from the Benfeito-1 well (the available well for this case study). Figure 4, summarizes the lithostratigraphy, for the study area, with the correlation of the seismic horizons interpreted ahead in this work, on Chapter 5-5.3. (blue – *Abadia Formation*, green – *Montejunto Formation*, yellow – *Cabaços Formation*, purple – *Brenha Formation*, orange – *Dagorda Formation* and red – *Grés de Silves*).



-Pre late Jurassic Units (LIAS)

On the Central Lusitanian Basin this pre late Jurassic Units comprise the Triassic Grés de Silves formation, the (Hettangian) Dagorda formation, the (Sinemurian) Coimbra formation and the lower (Pliensbachian) Brenha formation.

For the available well dataset the Benfeito-1 Well reached a total depth of 3343m, which is in the Dagorda formation. However from the seismic interpretation of the seismic lines dataset is possible to identify the top of the Silves formation. This is the oldest geological unit interpreted in the study area, below this interface the sediments are highly deformed, and we can consider this the Paleozoic Basement.

The Grés de Silves formation is composed of siliciclastic materials deposited in an alluvial fan environment under fault-controlled subsidence (Kullberg, 2000).

On the Benfeito-1 well report the Dagorda formation is characterized by brown argillaceous dolomites, with anhydrites and levels of mudstones, this can be explained by a period of sedimentation in the basin of a thick column of evaporites. The alternation of layers of clays, halite and anhydrite, is the result of deposition of sediments in shallow environments (like evaporitic lagoons or lakes) with inputs of salt water.

The Sinemurian Coimbra formation is, described has limestones, and dolomitic limestones, with some intercalations of dolomitic shales with oolites. The average thickness of this formation varies from 100m in the East, to 250m in the Western part of the sub-basin (Rocha et al, 1996). This unit was deposited in a progressively deepening marine, westerly dipping homoclinal ramp system (Kullberg, 2000). The average thickness of this unit is around the 200m on the two seismic lines.

The Brenha formation (Pliensbachian-Aalenian) is described on the Benfeito-1 Well report has a limestone, dolomitic limestone with some shales intercalated. This formation is associated with a deposition carbonate ramp setting of deep waters.

-Middle Jurassic Units (DOGGER)

The Candeeiros formation belong to the Middle Jurassic, however in some areas of the study are upper part of the Brenha formation is the geological lateral equivalent of the Candeeiros Fm.

For the top of the Candeeiros formation (Bathonian) is described has a microcrystalline limestones and sometimes fossiliferous limestones, in the middle part as an oolitic limestone, and in the bottom part of the unit (Bajocian) is dolomitic limestone.

When compared with Brenha Formation, Candeeiros Fm was also deposited on a carbonate ramp, but in a setting of shallow waters.

-Upper Jurassic Units

The Montejunto formation (Oxfordian) is a carbonate sequence with mudstones and marls, is characterized by a progressively deepening marine shelf environment (Leinfelder and Wilson 1998; Alves et al., 2002). There is the Cabaços Member from the Montejunto Formation, described on the Benfeito-1 well from the 1399-1585m. This is a carbonate-anhydrite sequence from a lacustrine depositional environment.

The lower part of the Abadia formation (Kimmeridgian) at approximately 1062-1136m of depth consist in a member called Cabrito that is a medium grained sandstone with limestone, marls and intercalations of grey silts and marls. But in general Abadia Formation is formed by a siliciclastic unit with an average thickness of 800m, from the infill of the Arruda sub-basin after the Late-Oxfordian and Early-Kimmeridgian rifting phase. On the top part of this formation, with 60-80m of thick is the Amaral oolitic carbonates. These carbonates consist of a shallow-water shelf carbonates coincident with a regressive episode.

At the top of the Jurassic in the Tithonian with 135m thick on the Benfeito well report, there's the pteroceriano unit which consists in sandstones with intercalations of mudstones and limestones.

Significant amounts of petroleum were generated in the Lusitanian basin as evidenced by the numerous surface manifestations and well shows, has reported in the Benfeito-1 well. (Lornholt *et al*, 1995).

In terms of petroleum systems there are, probably, two major ones in all the Portuguese basins. One, including a Paleozoic source rocks, Upper Triassic (or younger) reservoirs and Lower Jurassic (or younger) seals. This pre-salt petroleum system may be defined as sourced by meta-sedimentary Paleozoic rocks feeding upper Triassic siliciclastic reservoirs (Grés de Silves) and sealed by the Hettangian evaporitic clays (Dagorda formation,;Pena & Pimentel, 2014). On figure 5, is only represented the Triassic Reservoir from this pre-salt petroleum system, not the all system.

The second petroleum system, includes a Mesozoic source rocks and Mesozoic and/or Cenozoic reservoirs and seals, (Figure 5), corresponds to the maturation and oil generation of the transitional to coastal marine Kimmeridgian rift-related siliciclastics (Abadia and Lourinhã formations), entering the oil window in most of the basin since the early Cretaceous. This oil has abundantly impregnated the overlying Montejunto formation limestones and the Abadia formation, the seal for this kind of play could be Cretaceous and/or Tertiary clays and siltstones. (Pena & Pimentel, 2014) This system corresponds to the formations on the study area.

Mesozoic					
Triassic	Jurassic			Cretaceous	
Late	Early	Middle	Late	Early	
					Source Rock
					Reservoir
					Seal
					Overburden
					Trap
					Mat/Migr

Figure 5 - The Mesozoic Petroleum System chart adapted for the age of the units in the study area. *Adapted from Pena & Pimentel, 2014.*

Gonçalves et al, 2015 provide a study of the source rock potential in the Jurassic sequences of the Arruda sub-basin, the study taken into account data from the Benfeito-1 borehole, concluding that some intervals of Abadia, Montejunto, Cabaços and Brenha (Callovian age) Formations showed a good generative potential and can be consider as potential source rocks in the Arruda sub-basin. Abadia Formation has potential for gas generation while the remaining formations presented potential for generation of liquid hydrocarbons.

Taking this study and Pena & Reis, 2014) into account and knowing the formations of the study area (Figure 4), the early Jurassic source rock is the Brenha Formation, and the Late Jurassic are the Cabaços, Montejunto and Abadia, as can be recognized on figure 5.

3. Petrophysics

Log interpretation, or formation evaluation, requires the integrated interpretation of the logging tool response and geological knowledge, infer the maximum petrophysical information at the well location concerning subsurface formations. (Ellis & Grey, 2008)

Petrophysical log interpretation is one of the most useful tools to better understand and define the, subsurface physical rock properties such as lithology, porosity, pore geometry and permeability. A proper petrophysical may identify productive zones, and distinguish between the pore fluids *i.e* oil, gas and water within the porous space.

Well log data is acquired using different *Wireline* techniques such as, *Tough Logging Conditions*, *Measuring While Drilling (MWD)* and *Logging While Drilling (LWD)*.

Wireline is related to any aspect of logging that employs an electrical cable to lower tools into the borehole and to transmit data back to the surface. *Logging While Drilling (LWD)* and *Measuring While Drilling (MWD)* refers to wireline-quality formation measurements made while drilling. The logging sensors are imbedded in the drill collars used at the bottom of the drill string (near the bit). The *Tough Logging Conditions (TLC)* is used because in non-horizontal wells, is not possible to descend tools in flexible cables so when you get an “extreme” well, with some deviations and washouts, electrical cables carrying electrical signals are attached to the pipe. Therefore, the operations for this method are much longer consuming and difficult to perform.

One of the great advantages of the LWD in contrast of the normal well logging acquisition after the well has been drilled, is that the LWD can give real “semi-virgin” data from the formation in terms of petrophysical properties before being invaded by the perforation mud.

The petrophysical properties derived from the Benfeito-1 well logs under the scope of this thesis; are the porosity (\emptyset), bulk density (ρ_b), volume of shale (V_{sh}) and water saturation (S_w).

The theoretical equations for these properties, with the exception of the bulk density (the density of the entire formation, solid and fluid parts), which is directly taken from the RHOB well log curve.

- Porosity (Sonic derived porosity; *Wyllie et al. 1958*)

The sonic derived porosity was derived with equation 1.

$$\Phi_s = \frac{\Delta t_{log} - \Delta t_{ma}}{\Delta t_{fl} - \Delta t_{ma}} \quad (1)$$

The main log used to derive porosity is the sonic log, the interval transit time in the formation (Δt_{log}) dependent upon both the lithology and the porosity, and a formation's matrix interval transit time must be assumed (Δt_{ma}). Under the scope of this thesis Δt_{ma} was assumed $47.6 \mu sec/ft$ for a limestone, and finally the interval transit time in the fluid formation is assumed to be a freshwater fluid with a value of $189 \mu sec/ft$.

-Volume of Shale (from the Index of Gamma-Ray).

Shale is usually more radioactive than sand or carbonate, so gamma ray logs can be used to calculate volume of shale in porous reservoir.

$$I_{GR} = V_{shale} = \frac{GR_{log} - GR_{min}}{GR_{max} - GR_{min}} \quad (2)$$

The GR_{log} corresponds to the reading from the log, the GR_{min} , is the minimum value for the gamma ray log in this case for a clean sand or a carbonate, and the GR_{max} is the value for the maximum value, in this case a "spike" from a "shaly" zone.

-Water Saturation – Archie Equation

The water saturation is the amount of pore volume in a rock that is occupied by the formation water. In an exploration point the view the saturation that really matters, is the saturation in hydrocarbons (S_h). Water saturation is usually used because of its direct calculation in equations to determine the S_h as:

$$S_h = 1 - S_w$$

$$S_w = \left(\frac{a \times R_w}{\Phi^m \times R_t} \right)^{\frac{1}{n}} \quad (3)$$

Where (R_w) corresponds to the resistivity of the formation water, the R_t is the true formation resistivity as derived from the deep reading resistivity log from the uninvaded zone, which is the ILD (deep induction log) or LLD (deep laterolog), and of course the (Φ) is the porosity.

The (a, m, n) exponents represent the tortuosity factor, cementation exponent and saturation exponent respectively. The cementation exponent shows how much of the pore network increases the resistivity, as the rock itself is assumed to be non-conductive.

This relates the cementation exponent to the permeability of the rock, increasing permeability decreases the cementation exponent. The saturation exponent models the dependence of the presence of a non-conductive fluid (hydrocarbons) in the pore-space, and is related to the wettability of the rock. It can be assumed has equal to the value of the cementation exponent.

The tortuosity factor it is meant to correct for variation in compaction, pore structure and grain size.

For the calculation of this Archie Equation the most important set of logs is composed by the resistivity logs. Because the rock's matrix or grains are nonconductive and any hydrocarbon in the pores are also nonconductive, so the ability of the rock to transmit a current is almost entirely dependent of water (or brine) in the pores.

Generally speaking, as the hydrocarbon saturation increases (and the water saturation decreases) the formation's resistivity increases.

The values a, m, n for carbonates according to Carothers, (1968) and modified by Asquith, (1980) are 0.85, 2.14 and 2.14 respectively, the most commonly used is 1.0, 2.0 and 2.0.

4. Seismic Data

4.1 Seismic Reflection Method

Seismic Reflection method is probably the geophysical method most used among the oil and gas industry, mainly because of its potential in imaging the subsurface geology at great depths with high resolution. The seismic reflection data is the most important tool to look for potential hydrocarbon accumulations both onshore and offshore, because it allows not only the interpretation of the stratigraphy and structural geology of a given basin but also the quantification of the subsurface elastic properties.

The seismic method can be used in exploration, production and monitoring stages of a reservoir lifetime.

During the exploration stage seismic reflection data is used in the identification of the main *Leads* of the basin. Most of the times this is done recurring exclusively to regional 2-D seismic data.

In characterization and assessment, there's the risk assessment of the main *Leads*; and detailed interpretation and characterization of *Prospects* with depth estimation, petrophysical properties modeling and volume calculation.

In development, seismic reflection data may be used for quantitative subsurface characterization - seismic inversion and geological modeling; planning of the location and number of wells (producers and injectors) during production phase, and finally in monitoring with the 4D Seismic – OBS and OBC

Each seismic layer in the subsurface has its own acoustic impedance. The acoustic impedance is defined as, Equation 4:

$$AI = \text{density } (\rho) \times \text{velocity } (v) \quad (4)$$

The contrast between acoustic impedance is called reflection coefficient (RC), Equation 5:

$$RC = \frac{AI_2 - AI_1}{AI_2 + AI_1} \quad (5)$$

Seismic reflection data is generated by reflected energy at interfaces with contrasts in acoustic impedance. The recorded seismic data contains the travel-time between the source and its arrival at the receivers, in two-way travel-time (TWT). The two-way travel-time is defined as the time taken for the seismic waves to travel in depth from the source until they meet a boundary between layers with different Acoustic impedance, being reflected and returning to the surface.

The basic acquisition display for seismic data is formed by several geophones, aligned along a certain trajectory, recording data from the same shot. The geophones and shots are moved over the survey area to create a regular coverage of data points.

The seismic sources, generate the mechanical disturbances needed to cause a seismic wave motion with a characteristically “*signature*” to travel through the subsurface from the source to the receivers. On the Oil and Gas industry the most used in the onshore acquisitions which is the case for this thesis is the Vibroseis and Dynamite

The vibrator is a surface source and emits seismic waves by forcing vibrations from the vibrator baseplate which is kept in tight contact with the earth through a pulldown weight.

They are efficient, with less environmental impact for the populations near by the acquisition site and have a better control on the generated signal needed for the survey.

For the receivers in land the geophones are the most common ones, that convert seismic signal into an electrical signal, and record both the signal sent by the sources and reflected at the interface between lithologies, and also different types of any noise.

They are usually arranged in geometric (arrays) to improve the signal to noise ratio of the data, and can be receiver from more than 1 source at the same time.

In order to produce better results for the seismic interpretation, the raw data from the acquisitions surveys, need to be processed. The processing sequence aims improving the signal quality, signal to noise ratio, remove source effects, multiples, and display the seismic events in their correct position.

A typical processing sequence for a 2D survey consist in a preprocessing stage, which includes: demultiplexing, trace editing, spherical divergence and geometry corrections, and a processing flow which normally includes: deconvolution, Common Mid-Point (CMP) sorting, velocity analysis, normal moveout correction, CMP stack and migration (Azevedo, 2009), (Figure 6).

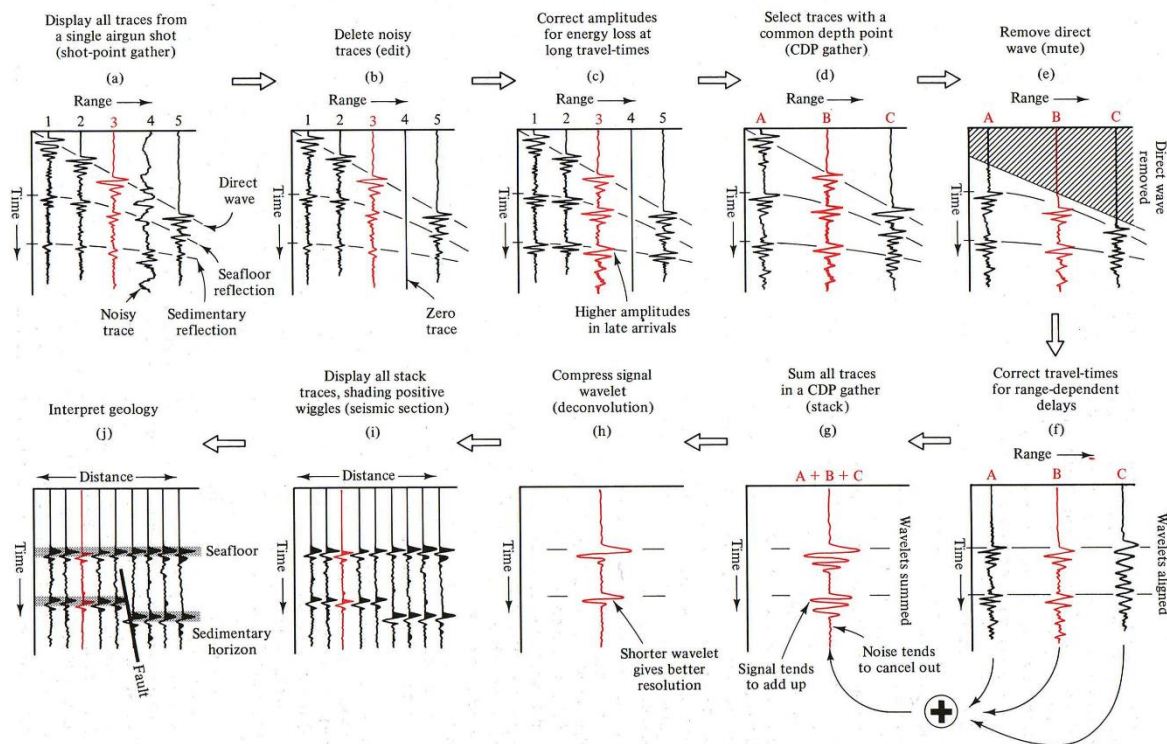


Figure 6 – Basic processing sequence for seismic data, adapted from Azevedo (2013).

One of the main steps during the processing sequence of the measured reflected signals is to sort the recorded data from the Shot into the Common Mid-Point domain (CMP).

CMP is a point at the surface located at half-offset between the source and the receiver, which is common to several source-receivers pairs. The number of times a CMP is sampled represents the *fold* of the data. A CMP gather is a collection of traces that share the same midpoint assuming a flat horizontal interface.

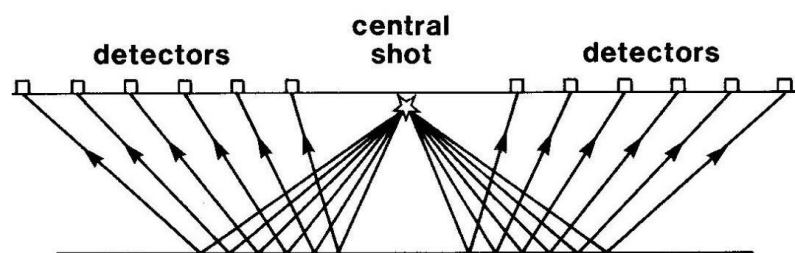


Figure 7 - Shot Gather for an onshore acquisition.

4.2 Seismic Interpretation

Many interpretations of the subsurface structure are based on seismic reflection profiles, provided by 2D or 3D seismic acquisition surveys. Mapping the main seismo-stratigraphic units has become key aspect for the Oil and Gas Industry, to find hydrocarbons accumulations and produced them in an efficient way. A detailed interpretation of the subsurface geology, allows reducing the risk of drilling an unsuccessful exploratory well.

The quality of the seismic interpretation depends of the seismic resolution of a certain survey. Resolution can be defined as the ability to distinguish between two objects which are located close to each other. Therefore, the vertical resolution is the minimum thickness to distinguish top and base of a formation; and lateral resolution can be defined as the ability to distinguish the lateral extent of the event.

The resolution of the seismic data may be increased by the seismic processing sequence applied to the raw data, to obtain a final and “good” section to be interpreted, and taking into account what can be noise or “artefacts” from the acquisition process.

The main point of seismic interpretation, is to identify seismic reflectors, correlated them with geological events, and provide a geological history, prospects identification and characterization.

Seismic interpretation should start in seismic sections perpendicular to the dip of the main structures, in areas of the basin with less deformation and from the deeper areas to the shallow ones; and in 3D seismic cubes, always marking more than one reflector at the same time and closing loops.

In terms of choosing the best seismic reflectors to start, they are related with the amplitude, and with the difference of lithologies, the ones with higher amplitudes are “strong” reflectors much easy to follow across all the seismic line.

Seismic units have different kinds of internal configurations, considered with stratification or without stratification (chaotic or reflection free). For the ones with stratification there is three types such has: *simple* (parallel, sub-parallel and divergent); *progradational* (sigmoid, shingled and oblique) or *complex* (hummocky, mounded and deformed) (Figure 8).

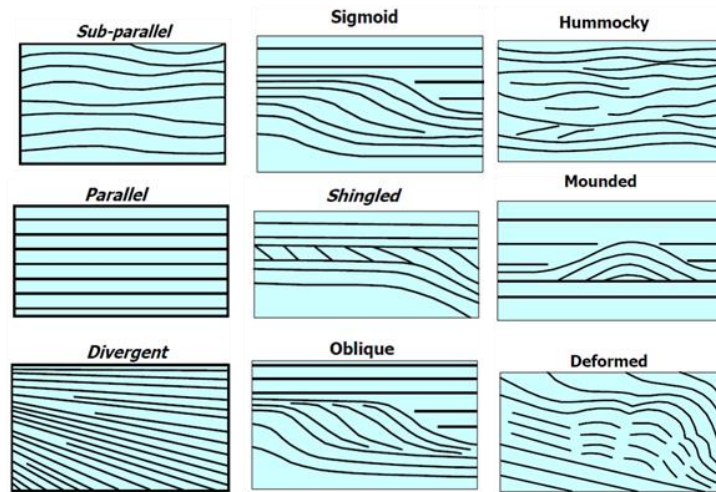


Figure 8 - The three types of reflectors stratification configuration, first for simple, second for progradational and third for complex.

Using the internal configuration of the reflectors seismic interpretation can be separated into two types, structural and stratigraphic.

The structural interpretation is related with the tectonic settings of the regional geology within the study area, and the stratigraphic interpretation is related to the main stratigraphic events in time, and the presence of a geological hiatus (time-gap) on the depositional column.

For the main tectonic settings, there is the extensional, compressive and strike-slip environments, these three types can generate structure able to the traps for hydrocarbon reservoirs, such as the propagation of faults and folds and salt tectonics.

For the stratigraphic interpretation the termination of the reflectors among another unit or the unconformity (disconformity, when parallel, or angular unconformity when the truncated data is presented with a different dip) between two units, can be a trap for the accumulation of hydrocarbons in terms of differences in the lithologies; of course this type of interpretation is highly dependent of a good knowledge of the main geological units and their age (chronostratigraphy) within the study area, and for this an exploratory well provide the information to the that type of correlation.

4.3 Seismic Inversion

The seismic inversion methods are used to infer subsurface elastic models from seismic reflection data, and are more and more commonly used by the Oil and Gas Industry both in Explorations and Production of hydrocarbons phases.

Most of the seismic inversion methods are based in a forward convolution of a reflectivity model with the estimated wavelet, comparison of the modelled output with the observed seismic trace and then updating the reflectivity model (inverting) to minimize the difference between the modelled and observed traces (Francis, 2006).

The advantage of using seismic inversion methods during the exploration phase can provide a better assessment of hydrocarbon accumulations for under-explored areas, *i.e.* with few available data, as well as better prediction of the petrophysical and fluid flow distributions during production phase.

Several techniques, both deterministic and probabilistic or stochastic, have been developed to solve the problem of seismic inversion and estimate the optimal reservoir model (Bosch *et al*, 2010).

Deterministic best-fit inverted models are low frequency and therefore can be considered as a smooth representation of the real and complex subsurface geology; In the deterministic approach, the more commonly used algorithms are the sparse-spike and model-based inversion (Bosh *et al*, (2010).

The stochastic seismic inversion can be described by the generation of several realizations of elastic properties, acoustic and/or elastic impedances and allow the assessment of the spatial uncertainty of those properties.

The match between observed and synthetic seismic is achieved by the maximization (or minimization) of an objective function that measures the mismatch between inverted and real seismic. Most often this measurement is a simply Pearson's correlation coefficient calculated between the synthetic and the recorded seismic reflection data (Azevedo, 2013).

In the scope of this thesis the inversion method used was a Global Stochastic Inversion (GSI) proposed by Soares, Diet, & Guerreiro (2007). According to the authors this GSI uses a global approach during the stochastic simulation stage, it's an iterative method that use the principle of cross-over genetic algorithms as the global optimization technique and where the model perturbation towards the objective function is performed recurring to sequential simulation and co-simulation.

According to Caetano (2009), the algorithm for this Global stochastic inversion can be defined by the next steps:

- Generate a set of initial images of acoustic impedances by using direct sequential simulation.
- Create the synthetic seismogram of amplitudes, by convolving the reflectivity, derived from acoustic impedances, with a known wavelet.
- Evaluate the match of the synthetic seismograms, of the image, and the real seismic by computing, for example local correlation coefficients.
- Ranking the “best” images based on the match (e.g. the average value or a percentile of correlation coefficients for the entire image). From them, one selects the best parts- the columns or the horizons with the best correlation coefficient – of each image. Compose one auxiliary image with the selected “best” parts, for the next simulation step.
- Generate a new set of images, by direct co-simulation, and return to step 2, until a given threshold of the objective function is reached.

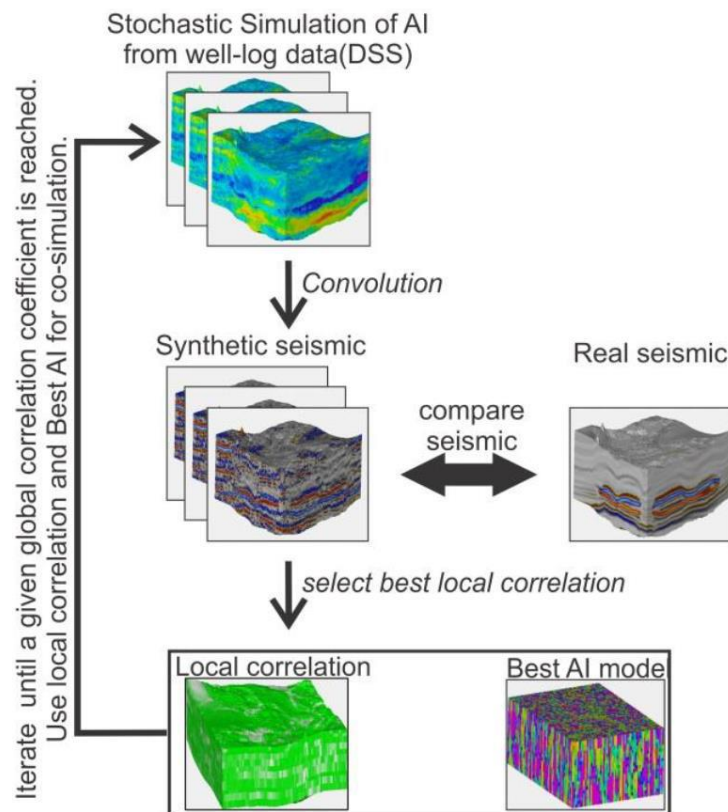


Figure 9 - Schematic representation of the Geostatistical Seismic Inversion; Adapted from Azevedo, (2013)

5. Case Study

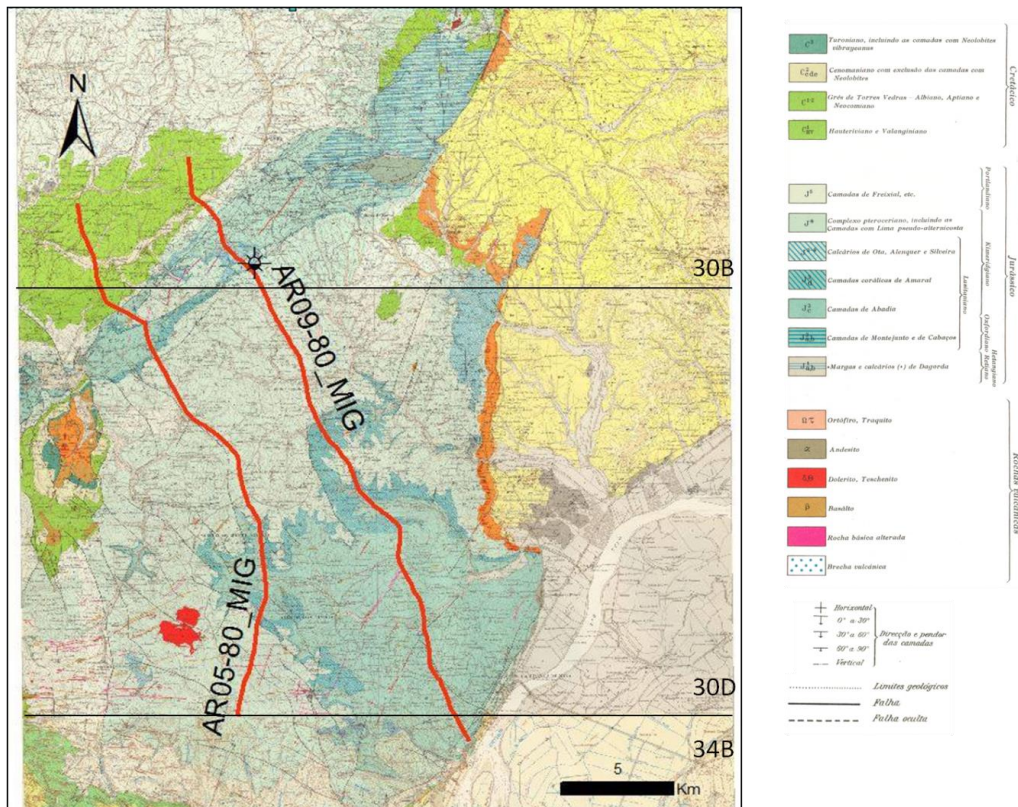
This chapter comprises the description of the available real dataset used under the scope of this thesis and the main results achieved by the integrated interpretation of seismic, well-log and the inversion results. This dataset was kindly provided by the UPEP - Unidade de Pesquisa e Exploração de Recursos Petrolíferos from ENMC, for this study.

5.1 Data-set

The available dataset for this study is located in 3 Geological Maps of Portugal, in the scale of 1:50000, of 3 areas: 30-B – Bombarral, 30-D Alenquer and 34-B Loures (Figure 10).

Evidences of halokinesis and halite has a mineral resource are recorded on the Notice of each of this 3 Geological maps on the areas belonging to the Bombarral and Turcifal Sub-basins in units from the Early Jurassic. In the study area (Arruda Sub-basin), there are no evidences of any diapiric structures.

Geologically according to Wilson (1988) where the Dagorda Formation is thick, diapiric structures developed over reactivated Hercynian basement faults, but where this formation is thin, the faults propagated into younger sediments which is the case on the Arruda Sub-basin study area.



The data-set interpreted in this thesis, is composed by: two, 2D seismic lines (AR09_80-MIG and AR05_80-MIG), and 1 well (Benfeito-1), (Figure 11).

These seismic lines are part of the seismic survey named PETROGAL 80, acquired during 1980-1981, with 35 lines, 2682 shot points and total length in km of 724,6.

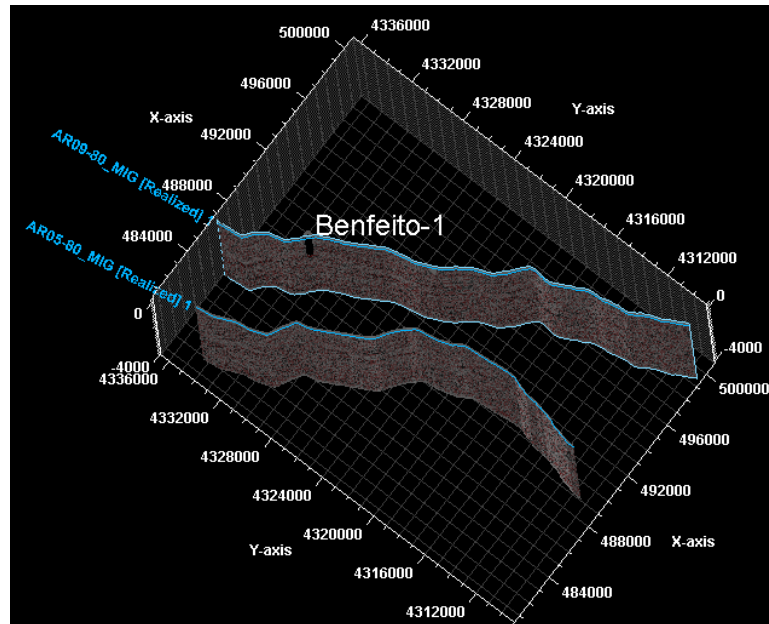


Figure 11 - Location of the (AR09_80-MIG and AR05_80-MIG) seismic lines plus the location of the Benfeito Well

The Benfeito-1 well was drilled in 18 November 1982; the location is on Quinta da Boavista, on 750 m NW from the population of Parreiras. Its location is within a radius of 100 meters from the Seismic Line AR9-80_MIG, and the total depth of the well is 3343 m.

The formations drilled along the well were 8, but in terms of seismic correlation, with the two 2D seismic lines of this data set, only 6 formations can be followed on the seismic reflectors, one of them corresponding to the basement.

In terms of well logging, the logs acquired started at 998 m of depth which correspond to the final part of the Abadia Formation. The main logs used to better understand the formations and characterized in a petrophysical way were; Caliper (CALI), Gamma-ray log (GR), Sonic-log (DT), Density-log (RHOB), Neutron-log (NHPI), Spontaneous Potential (SP), Microspherically focused-log (MSF), Deep Latero-log (LLD) and Deep Induction-log (ILD), as an example given in figure 12.

5.2 Petrophysical Analysis

The petrophysical data computed under the scope of this thesis is mainly representative of the Abadia and Dagorda Fm. This fact is related with the available logs started at 998 m of depth which correspond to the final part of the Abadia Formation, ending at 3273m, which corresponds to a middle part of the Dagorda Formations.

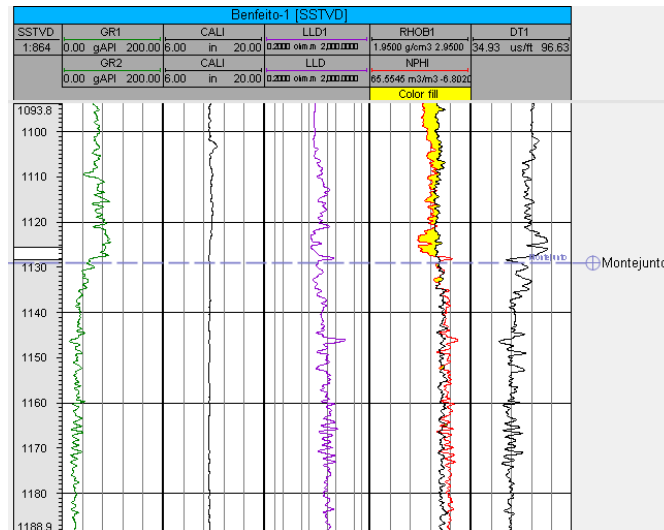


Figure 12 - Example of the well logs presented on the Benfeito-1 well.

The well-log reports show indications of hydrocarbon on some of the stratigraphic units such as; Abadia Formation, Montejunto Formation, Dogger and Lias, at the depth of: 900-100m; 1270-1370m; 1500-1600m; 1750-2550m and 3094-3150m, they are identified with “stars”, (Figure 13).

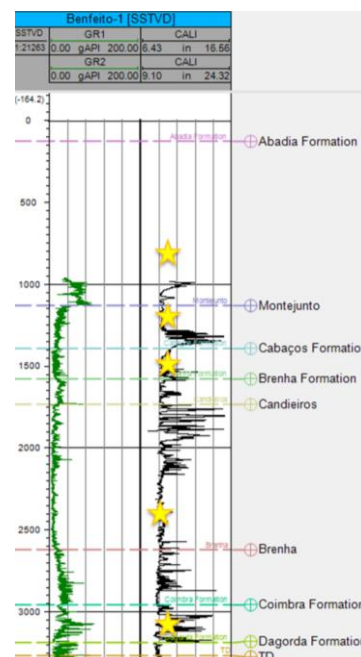


Figure 13 - Benfeito-1 Well Tops, and “reservoir” areas has “stars” on the report.

The geological units characterized in terms of the petrophysical properties, are summarized in the next image in terms of: Volume of shale (Equation 2), Porosity (Equation 1), Bulk density and Water saturation (Equation 3). The seismic horizons presented in this table, correspond to the ones interpreted on the two seismic lines (Figure 14).

Depositional Units	Seismic horizons	Depth(m)	Vshale (%)	Porosity (%)	Bulk Density (g/cm ³)	Sw (%)
<i>Abadia Formation</i>		135-1137m				
<i>Montejunto Formation</i>		1137-1399m	20	5,64	2,5631	77,70
<i>Cabaços Formation</i>		1399-1585m	12	2,17	2,7231	39,80
<i>Brenha Formation (Callovian)</i>		1585-1740m	23	5,77	2,6195	59,23
<i>Candeeiros Formation</i>		1740-2627m	7	1,79	2,6446	89,78
<i>Brenha Formation (Aalenian-Pliensbachian)</i>		2627-2963m	25	3,17	2,7008	69,24
<i>Coimbra Formation</i>		2963-3194m	27	3,03	2,6448	66,55
<i>Dagorda Formation</i>		3194m-				

Figure 14 - Summary of the values obtain for different petrophysical parameters for the main units

In terms of volume of shale, Candeeiros Formation is the one that present the lower value, due to the fact that is a dolomitic limestone. All the other formations present intercalations of shale and silty material increasing the value for the volume of shale. The Cabaços Formation is the formation with the lowest value of water saturation, 39.80%. This value was computed following equation 3. The bulk density is directly related with the type of lithology, and the values are according to the lithologies present on each formation.

In case of porosity, the values presented on the table (Figure 14), correspond to the average value, calculated, for each unit individually. The porosities in these units are very low, this has been described on the well report for Benfeito-1, but if we look in detail, by plotting the sonic-log derived porosity versus the depth for each unit, we can infer some zones of interest with higher values of porosity.

For Montejunto Formation, which includes the Cabaços Formation as a member (Figure 15), at the top near 1137m depth have higher values of porosity (6-12%) comparing with the deeper part of the unit (Cabaços Member), between 1387m and 1585m, where the porosity values are around 2%.

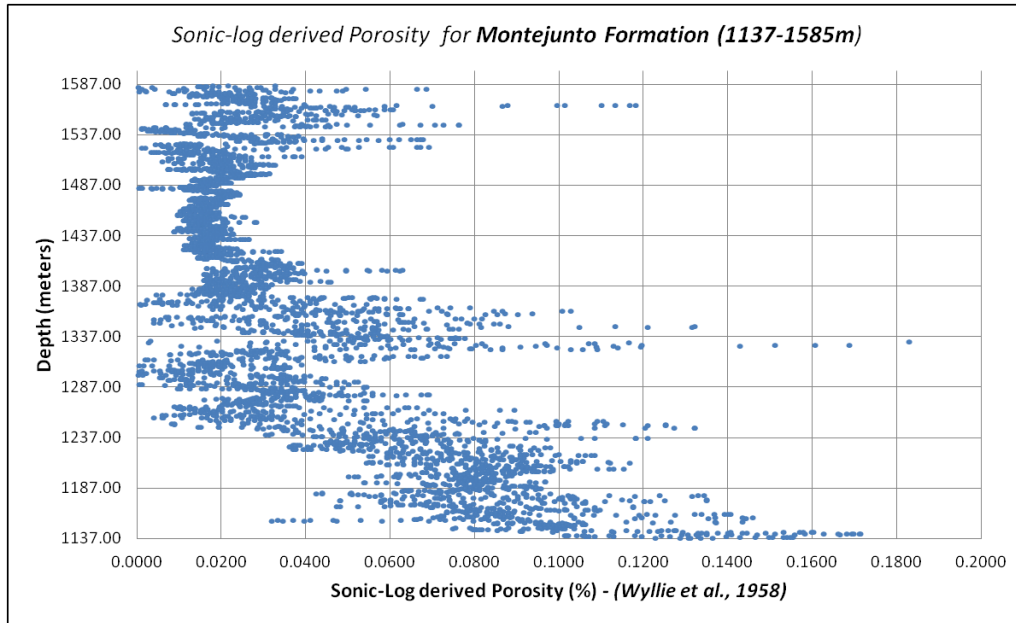


Figure 15 - Sonic-log derived Porosity (Wyllie *et al.*, 1958) for Montejunto Formation

For Brenha Formation (Callovian; Figure 16) the values of porosity are more or less around 4% to 8%, and does not present a very distinct distribution along the depth.

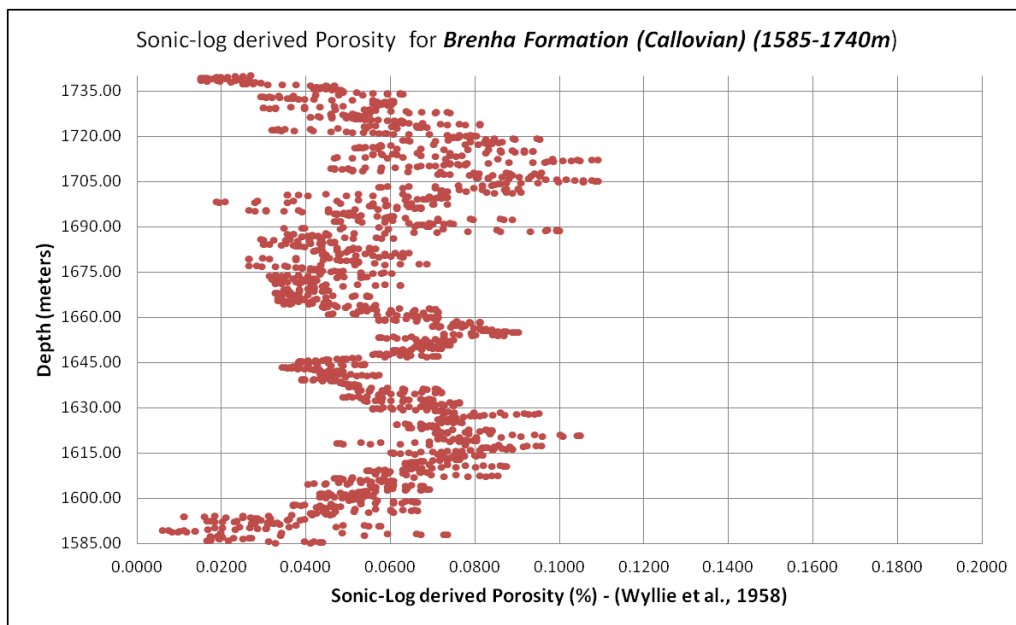


Figure 16 - Sonic-log derived Porosity (Wyllie *et al.*, 1958) for Brenha Formation (Callovian)

For Candeiros Formation (Figure 17) the values of porosity present a very regular distribution along the depth, but the values vary between 0% to 4%. This lower values can be explained by the fact this formation has a oolitic and bioclastic component and in order of its size, that can decrease the values of porosity; and that's way this unit present the lowest value of porosity – 1,79%.

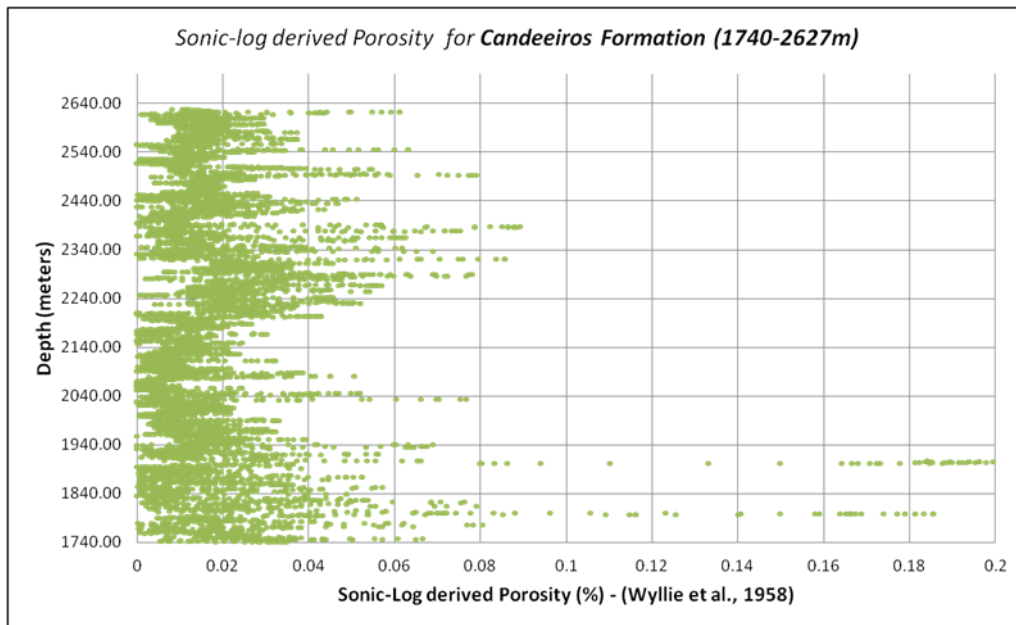


Figure 17 - Sonic-log derived Porosity (Wyllie *et al.*, 1958) for Candeiros Formation

For Brenha Formation (Aalenian-Pliensbachian; Figure 18), the values of porosity range between 2% to 6%, there is a tendency to present higher values in deeper areas, near the 2920 m.

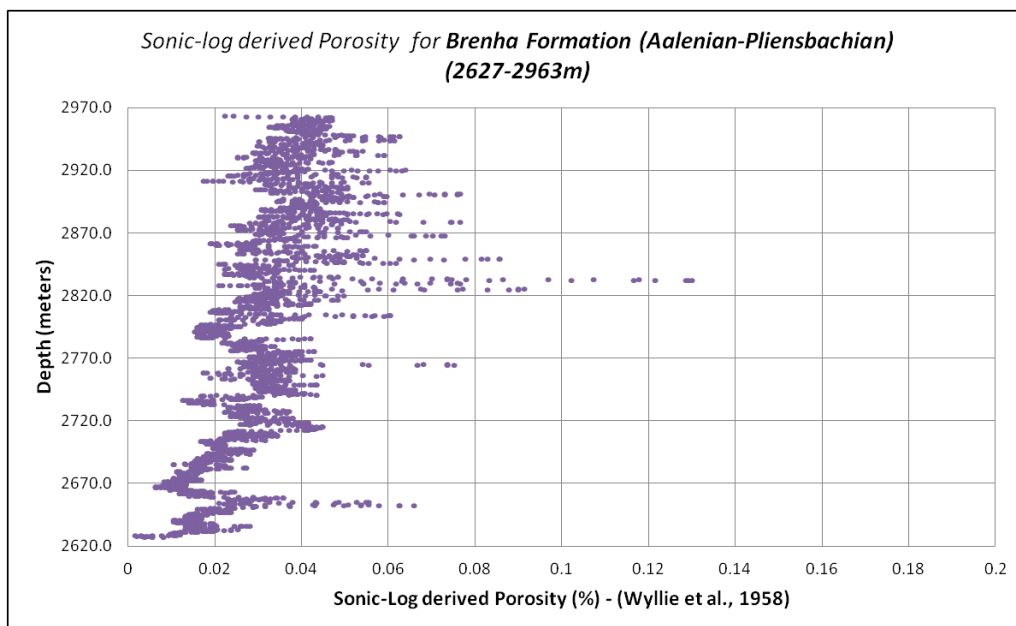


Figure 18 - Sonic-log derived Porosity (Wyllie *et al.*, 1958) for Brenha Formation (Aalenian-Pliensbachian)

For the Coimbra Formation (Figure 19) the values of porosity present better results on the top of the unit, (2963-3060m), around 2% to 4%, when compared to the lower part in depth that are very near 0%.

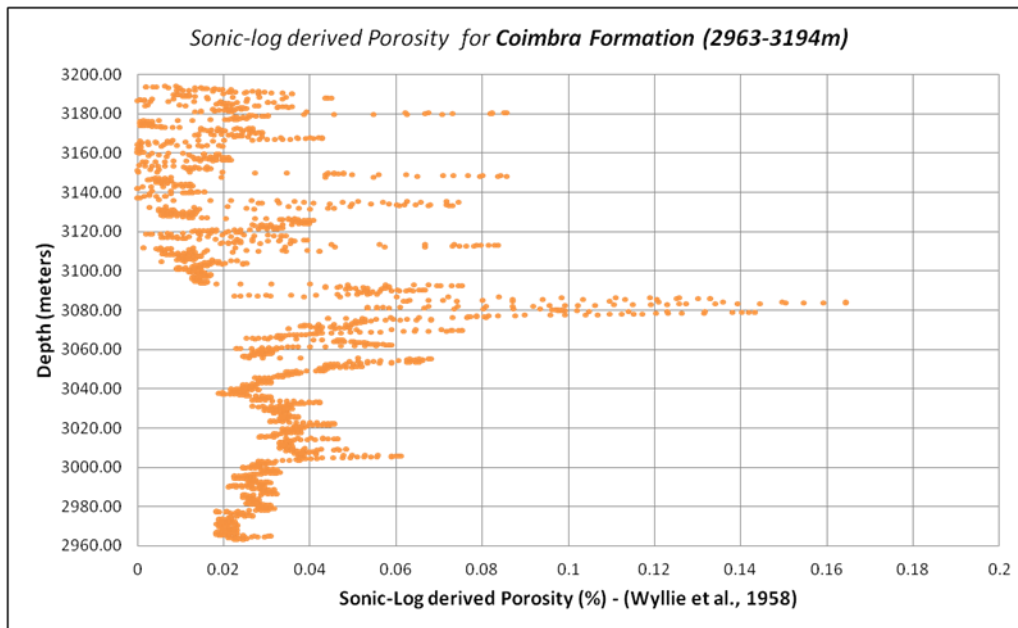


Figure 19 - Sonic-log derived Porosity (Wyllie *et al.*, 1958) for Coimbra Formation.

This preliminary petrophysical analysis show that there is a real potential, in terms of porosity values, for reservoir rocks mainly in the Brenha and Montejunto formations.

5.3 Seismic Interpretation

The seismic line AR05_80-MIG (Figure 20 and 21) has a challenging flower structure partly deformed, hard to interpret with low signal-to-noise ratio. There is no well tie to this seismic line, and the interpretation was heavily based on the interpretation made for the AR09_80-MIG seismic line, which is located close to the available well. In the fact, the two seismic lines are parallel to each other (Figure 11). In this way, the assumption behind the interpretation process was such that the interpreted horizons and faults are as much spatially correlated as possible between the two seismic lines.

For the seismic line AR09_80-MIG (Figure 22 and 23) there were already some interpretations published by other authors. About the accuracy of that interpretations it is hard to make an argument based exclusively on the available dataset for this study. Mainly due to the poor quality seismic reflection data with seismic reflectors very difficult to follow, and the flower structure in the middle of the structure probably generated due to the movement of the salt.

For this thesis the re-interpretation of the AR09_80-MIG was done by inserting the well tops from the Benfeito-1 well that was previously tied to the seismic and following the main stronger reflectors that correspond to the main seismic units.

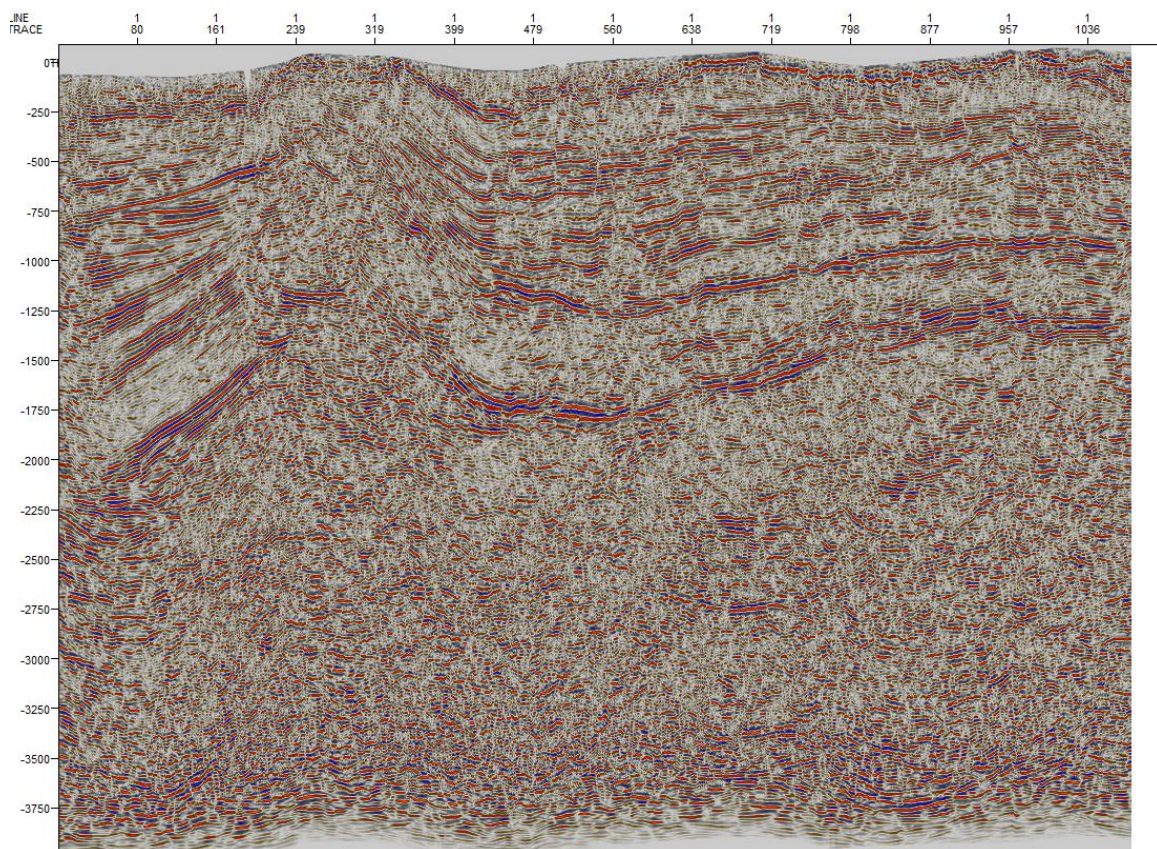


Figure 20 - AR05_80-MIG Seismic Line.

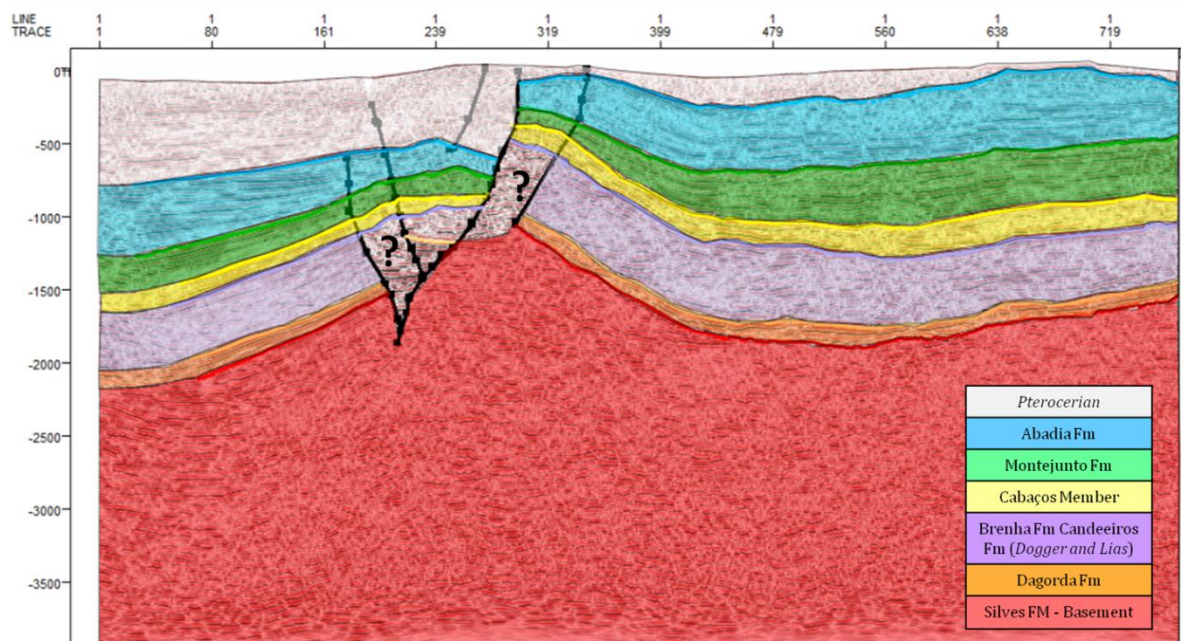


Figure 21 - AR05_80-MIG Seismic Line interpreted.

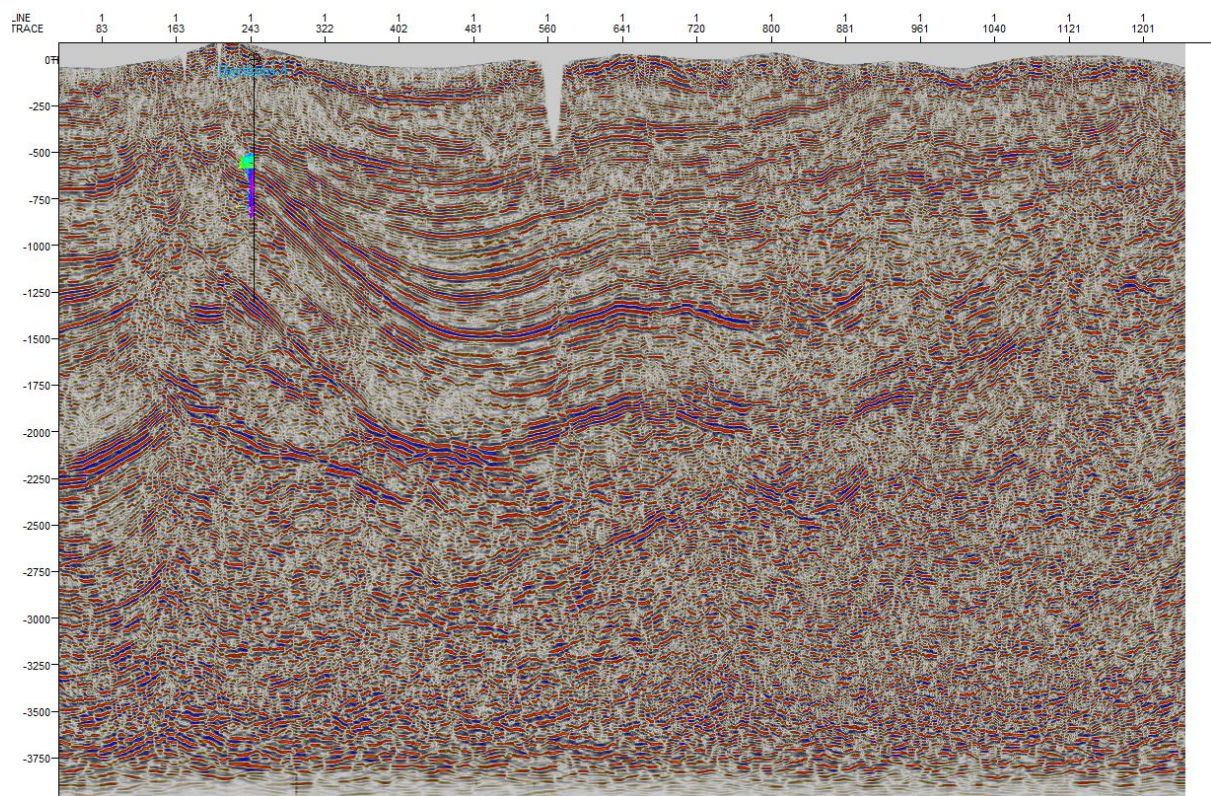


Figure 22 - AR09_80-MIG Seismic Line.

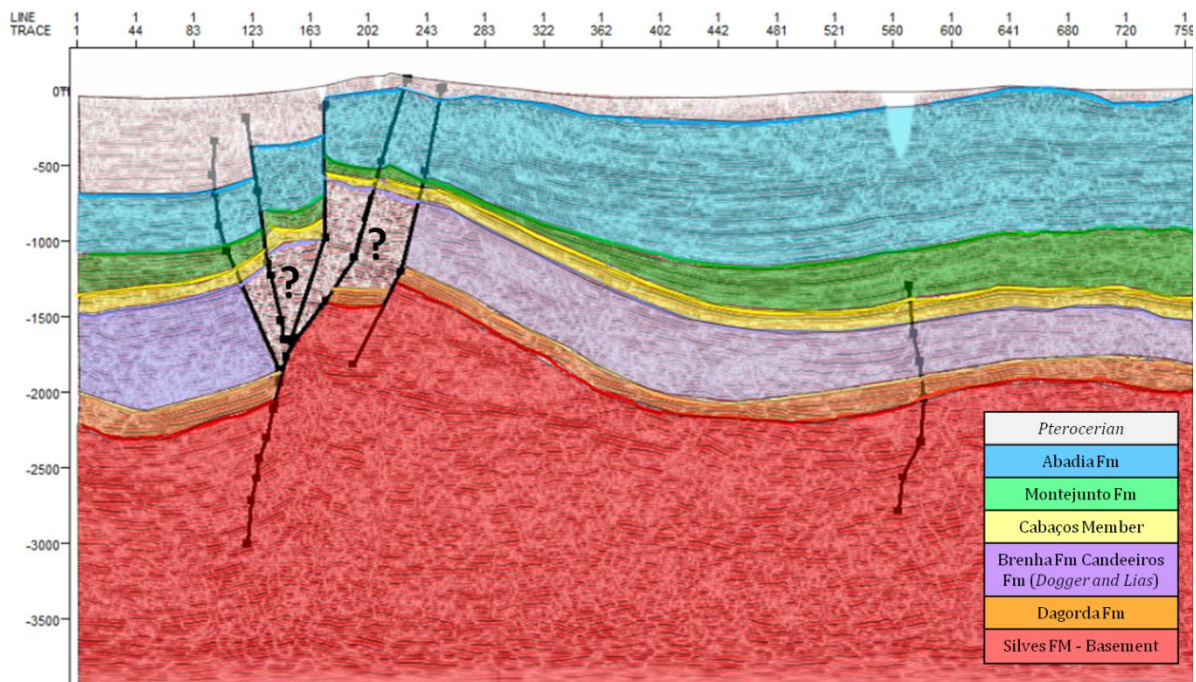


Figure 23 - AR09_80-MIG Seismic Line interpreted.

From the seismic interpretation of both seismic lines, we may say that the most important structural event is the presence of a flower structure which is a folded structure associated with strike-slip faults. In areas where strike-slip faults occur in converging crust, or transpression, rocks are faulted upward in a positive flower structure. In areas of strike-slip faulting in diverging crust, or transtension, rocks drop down to form a negative flower structure. Flower structures can form hydrocarbon traps. The term "flower structure" reflects the resemblance of the structure to the petals of a flower in cross section.

It's difficult to follow the reflectors in both lines on the center of the faulted area, the seismic is very chaotic due to the movement of salt, and the reactivation of the Hercynian basement faults. This complex geological framework results in a poor signal-to-noise ratio of these seismic lines for this particular area.

Nevertheless, the Grés the Silves Formation, also considered Basement (red section of the lines), has not been confirmed by drilling, it's being assumed that the top of the Triassic is a strong reflector found at the what has been assumed has the base of the massive salt from the Dagorda Formation, once the total depth of the Benfeito-1 well does not correspond to the top of the Dagorda Formation.

All the others formations are present as well tops for the Benfeito-1 Well. These well tops were followed along the seismic lines with the exception of the Candeeiros Formation and Coimbra Formation (Dogger and Lias) and it was decided to include them as part of the Brenha Formation. The reflectors were very poor in terms of amplitude, so following them would result in a high degree of uncertainty.

Notice that for this thesis, the interpretation was only based on the well tops from the Benfeito-1. Following the reflectors along the line to the southern part, which also appears highly deformed with low signal-to-noise ratio is not easy. Therefore, and based exclusively on the available dataset we decided

to follow the reflectors in order to keep the thickness of the seismic units. However, this simplified interpretation may not be strictly matching the knowledge of the subsurface geology.

This AR09_80-MIG seismic line is located next to the Benfeito-1 well. However, near this seismic line, there are other exploratory wells presented along the line from North to South, *Aldeia Grande-2*, *Benfeito-1*, *Freixial-1*, *Arruda-1* and *Montalegre-1* (not available for this study). The subsurface geology is so complex, that the MILUPOBAS report which takes into account all the well tops from all the available wells in this basin, shows a high uncertain interpretation in both the fault and horizon interpretation.

The MILUPOBAS report (Figure 24) has a interpretation of the following horizons: the Horizon 7, corresponding to Abadia Formation, Horizon 9, Montejunto Formation, Horizon 10, Cabaços Formation, Horizon 11, Brenha Formation, Horizon 13, Coimbra, Horizon 14 – Dagorda Formation, Horizon 15, Grés de Silves and finally Horizon 16 the Basement.

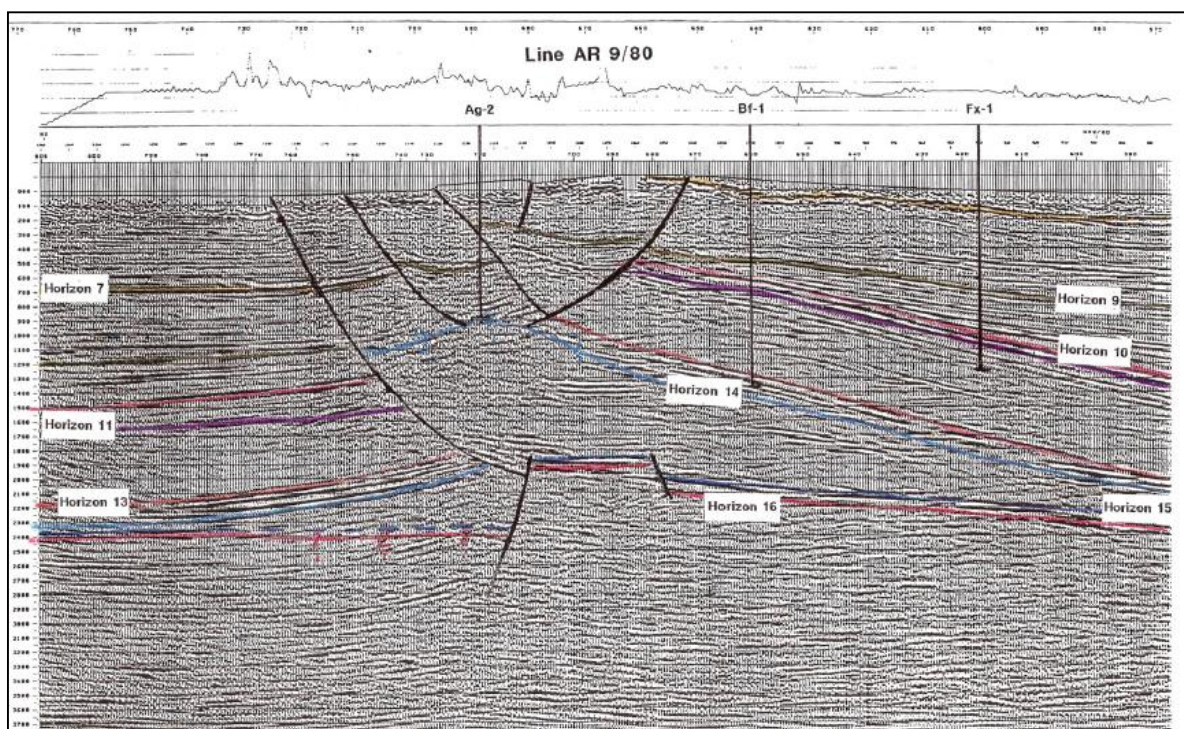


Figure 24 - Interpretation of AR09_80-MIG Seismic Line, from the MILUPOBAS report.

The main challenges of the interpretation of this line are related with the good delimitation of the end of the Grés de Silves Formations, because all the seismic section under this strong reflector is deformed and this has not been confirmed by drilling.

Second, one of the main differences between this interpretation and the new re-interpretation, are related with the faulted area, in this case is considered a listric fault, with the top of the Dagorda Salt, presenting a diapiric structure for this formation, with reactivated faults from the salt movement, and at the end of the listric fault, a horst structure delimited with normal faults on the top with the Grés de

Silves and for the Basement tops. Above this diapiric structure is all considered has Montejunto Formation, Horizon 9, with no indication from continuity in the Abadia Formation, from one side to another of the reactivated faults of the diapir

The re-interpretation presented in figure 23, makes more geological sense to consider one main fault from the basement to younger sediments on a flower structure, because on the supposedly diapiric structure (Figure 24) they assumed the reflector continuous for the Dagorda Salt, with a dome geometry, on a section that is clearly discontinuous, with indications of fault planes on the seismic.

In thickness terms, for the Dagorda and Abadia Formation is obviously very different from Figure 23 to Figure 24; for the other horizons is almost the same, but of course this is explained by the assumptions done for the re-interpretation done under this thesis.

For the geostatistical seismic inversion (Chapter 5- 5.4), the reflectors were followed straight forward to south of the AR09_80-MIG, and AR05_80-MIG seismic lines, keeping as possible the same thickness for each unit. In geological terms, with the information referred by several authors and presented on the interpretation from the MILUPOBAS report, on the Arruda-1, they drilled 2137m of the Abadia Formation, (Figure 25).

This is very inconclusive taken into account that the Benfeito-1 well has a total depth of 3273m, it's fairly strange the Abadia Formation has a thickness almost the size of the total depth of the Benfeito-1 well; another proof is the nearby Montalegre-1 well proved to present a very similar sequence to Benfeito and entering the Hercynian Basement at 1714.5 m of depth.

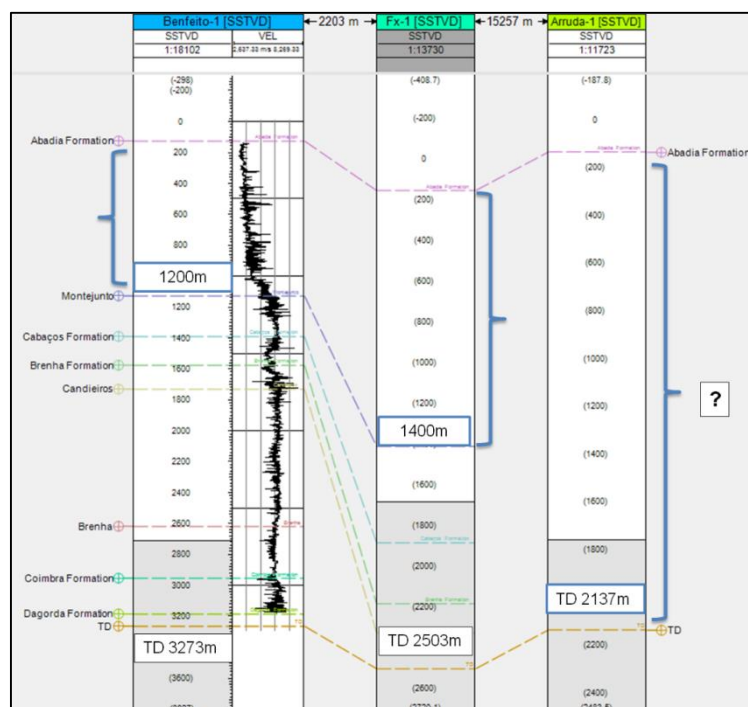


Figure 25 - Projection of the Benfeito-1 Well, Frexial-1 Well and Arruda-1 Well, showing the huge variation in thickness for the Abadia Formation on the southern part of the Seismic Line AR09_80-MIG.

For the Montejunto formation and for the AR09_80-MIG seismic line is important to refer the truncation in onlap of some of the reflectors, which makes a stratigraphic trap, on the case of hydrocarbons exploration, but on the AR05_80-MIG the reflectors of this formation don't present this kind of geometrical configuration.







Depositional Units	Seismic horizons	TWT thickness (ms)	Internal configuration, continuity & amplitude strength	Internal configuration, continuity & amplitude strength
<i>Abadia Formation</i>		18.0-544.0	Sub-parallel to wavy, semi-continuous to discontinuous. Low to moderate amplitude on the top and moderate to high amplitude on the lower part.	Sub-parallel to wavy, semi-continuous to discontinuous. Moderate amplitude.
<i>Montejunto Formation</i>		544.0-644.0	Sigmoide configuration, there is a truncation in onlap of the reflectors. Sub parallel to wavy, semi-continuous. And the amplitude is moderate to low.	Sub-parallel to wavy, semi-continuous. Low to moderate amplitude.
<i>Cabaços Formation</i>		644.0-704.0	Parallel and semi-continuous. The amplitude is moderate to low.	Sub-parallel to wavy, semi-continuous. Low to moderate amplitude.
<i>Brenha Formation</i>		704.0-1158.0	The configuration is wavy to sub-parallel, but on the lower part we can consider shingled. Semi-continuous reflectores and moderate to low amplitude.	Wavy configuration, discontinuous, and low amplitude almost reflection free in some areas of the seismic section
<i>Dagorda Formation</i>		1234.0-1266.0	Sub-parallel to wavy. Mounded on certain parts of the seismic section. And the reflectors have a high amplitude.	Sub-parallel to wavy. Mounded. And the reflectors have a moderate to high amplitude.
<i>Grés de Silves (Basement)</i>		1266.0-	Wavy to hummocky configuration. The reflectores are very discontinuous and the amplitude is moderate to high.	Wavy to hummocky configuration. The reflectores are very discontinuous and the amplitude is moderate to high.

Figure 27 – Summary of the main horizons interpreted and the analyses based on internal configuration, continuity and amplitude strength, for the AR09_80-MIG and AR05_80-MIG Seismic lines.

After the interpretation of the same units on the two seismic lines, a polygon was created along the lines, in order to make surfaces for each unit. The surfaces were converted from TWT into depth using an interval velocity value for each formation. The goal was to obtain isopachs maps in thickness (meters) of the area. The values for the velocity of each formation were obtained from the well report Benfeito-1.

The horizons interpreted are six but the isopachs (Figure 27) created are only five, because in the case of the last unit considered (Grés de Silves Formation- Basement) there's no velocity information of the Benfeito well logs, due to the total depth correspond to the middle of the formation above (Dagorda Formation) (Figure 26).

The velocities used from the most recent unit to the oldest are:

Abadia Formation – 3809 m/sec;

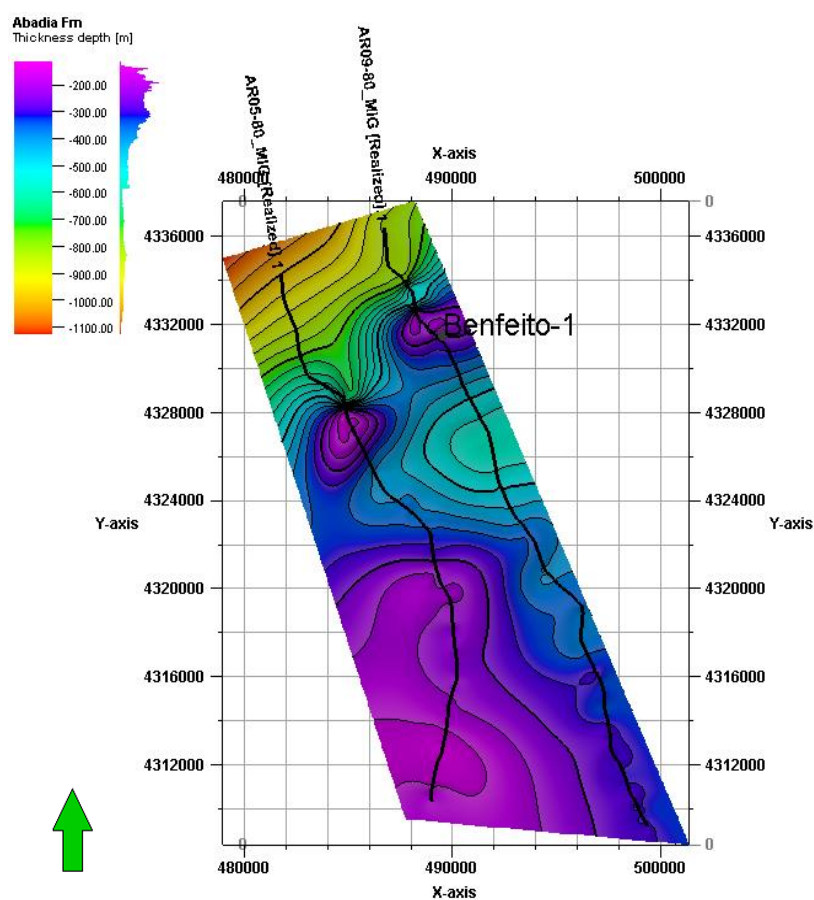
Montejunto Formation – 5240 m/sec;

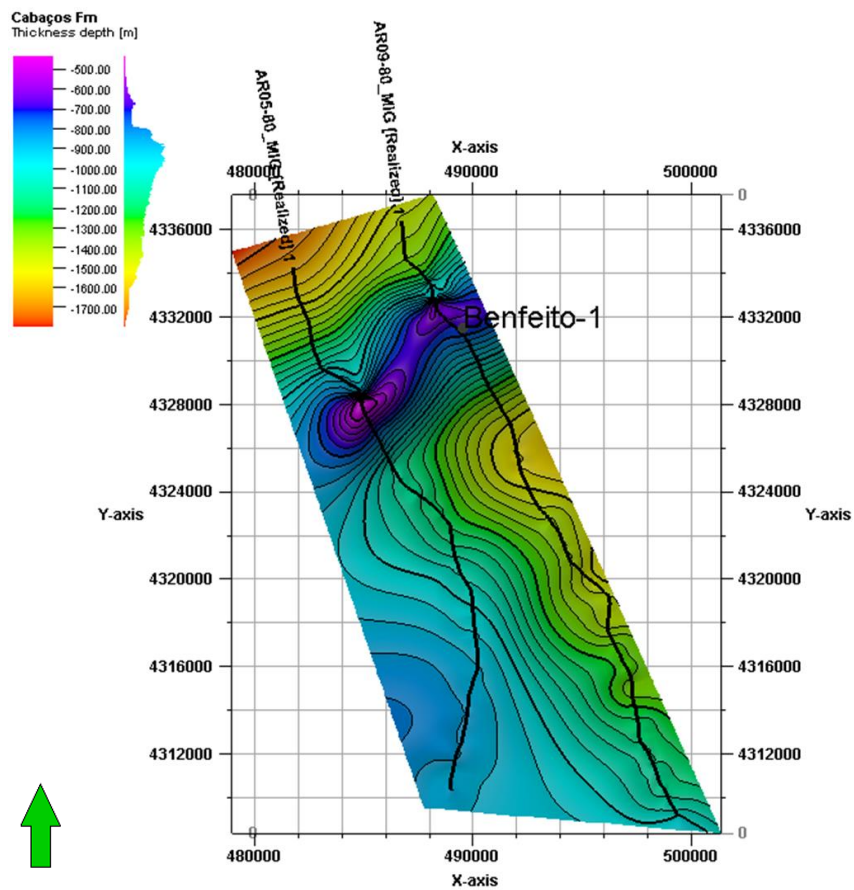
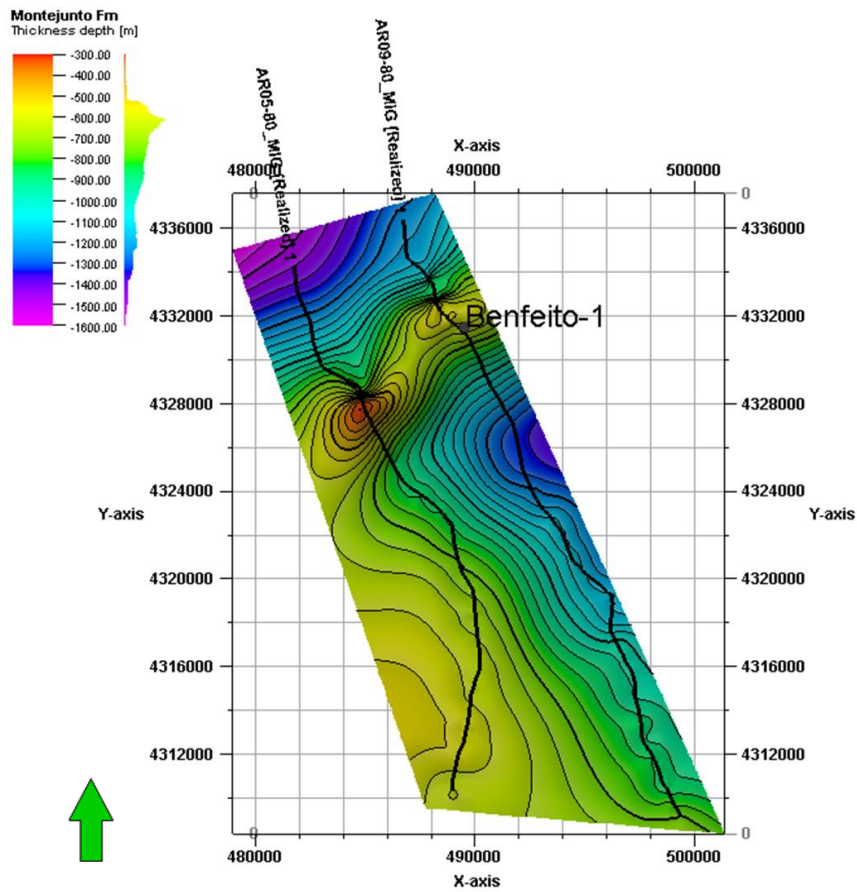
Cabaços Formation – 6200 m/sec

Brenha Formation – 5961m/sec

Dagorda Formation – 4937m/sec

As concluded above in this thesis, the isopach maps are highly uncertain due to the lack of seismic lines, mainly for the southern part of the region due to the issues previously discussed. But on the faulted north section of the seismic lines, near the Benfeito-1 well, we can infer that the formations thicknesses are: Abadia Formation thickness varies between 200m to 1100m, the Montejunto Formation between 300m to 1600m, Cabaços Formation between 500m to 1700m, Brenha Formation between 800m-2000m and finally Dagorda Formation 1100m to 2300m. (Figure 18).





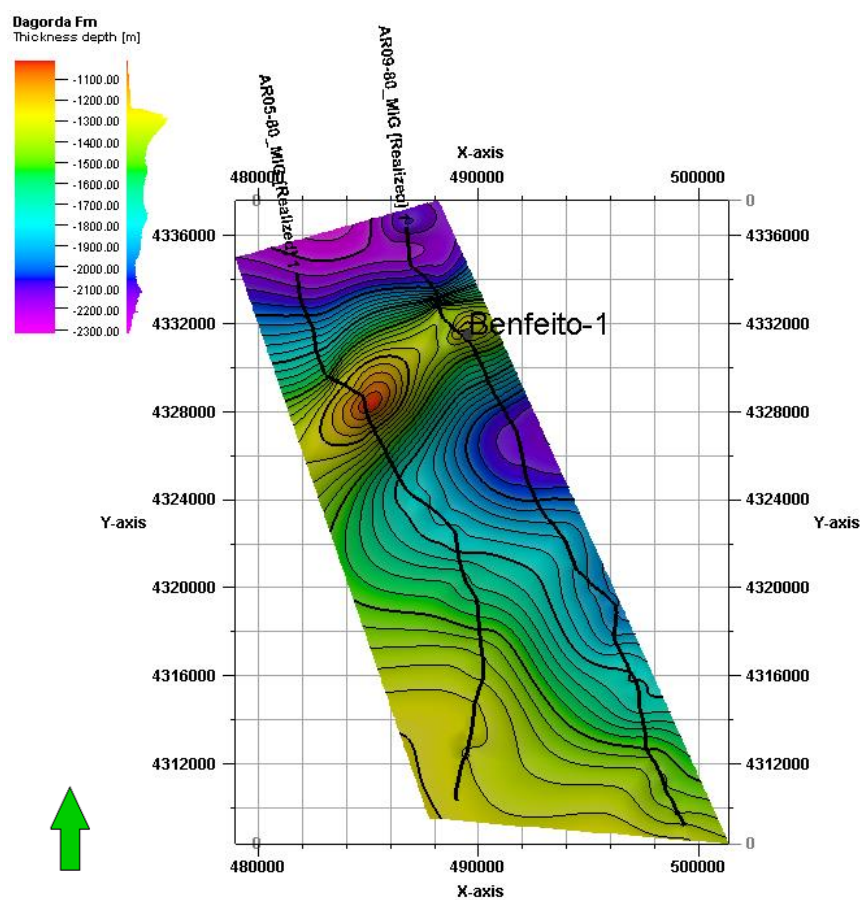
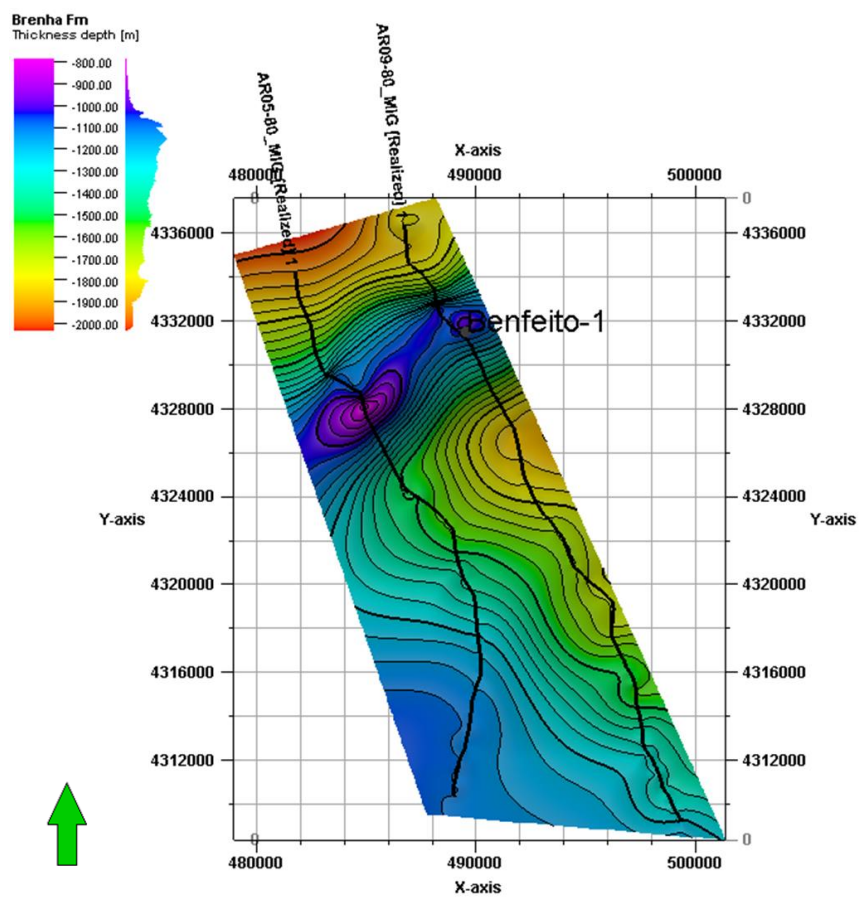


Figure 28 - Isopachs for Abadia Fm, Montejunto Fm, Cabaços Fm, Brenha Fm and Dagorda Fm, respectively.

5.4 Seismic Inversion

The objective of this chapter is to apply a Geostatistical Seismic Inversion (GSI) to the AR09_80-MIG and AR05_80-MIG 2D seismic lines using the hard-data from the Benfeito-1 Well, in two ways; one is the regular GSI, and other constraining each layer with a given conditional distribution per zone as interpreted from the seismic reflection data.

First of all, the two seismic line AR09_80-MIG and AR05_80-MIG were cropped taking into account the most interesting part of the seismic lines, and where the Benfeito-1 well was drilled. Each inversion grid as the following size 1-245-501 cells and 1-1081-501 respectively for each seismic line.

For both cases, with and without zones, the results of the (GSI) presented in this work were obtained from 32 Simulations with 6 iterations.

Following will be presented the first iteration, 1 simulation **(1-1)**, the third iteration, 17 simulations **(3-17)** and finally the sixth iteration, 32 simulations. **(6-32)**. The corresponding best correlation volumes of the first, third and sixth iterations are also showed in order to assess the convergence of the inversion methodology, for the application of the GSI by zones.

Presented next are 3 results obtain from a GSI without zones for the **AR05_80-MIG seismic line**. (Figures 29, 30 and 31).

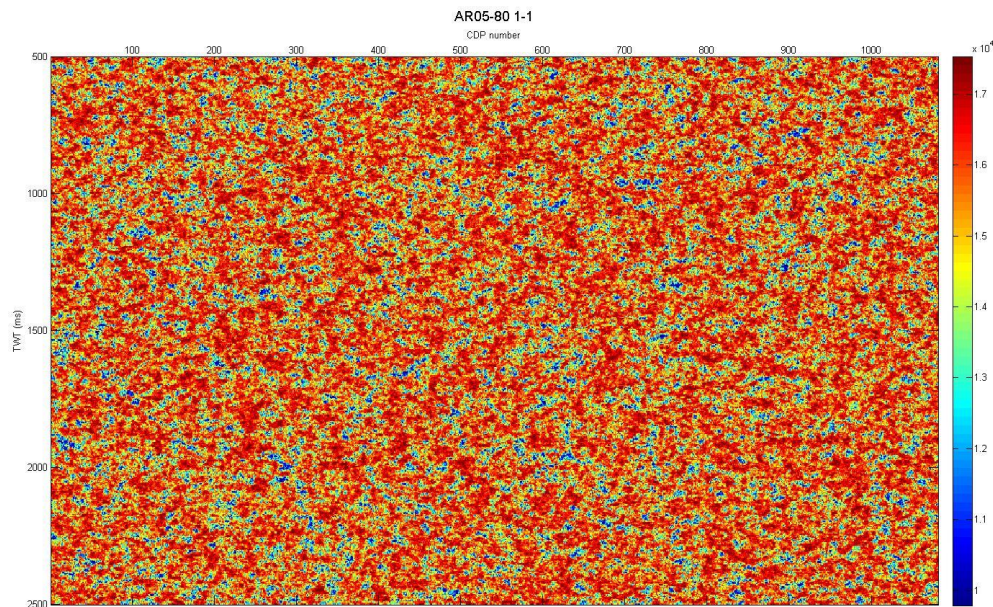


Figure 29 –Result form (1-1) case for the GSI for AR05_80-MIG seismic line.

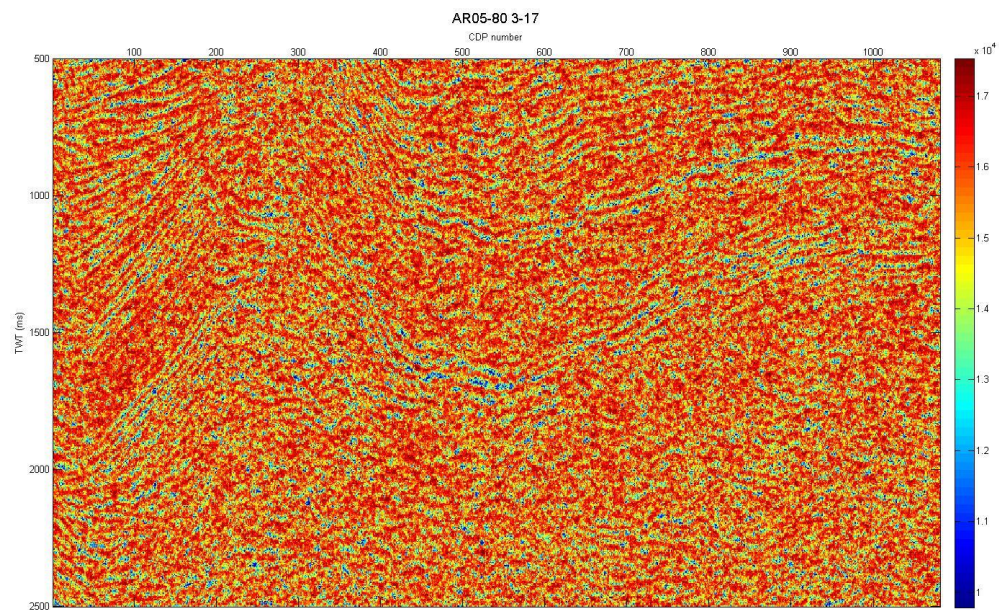


Figure 30 - Result form (3-17) case for the GSI for AR05_80-MIG seismic line.

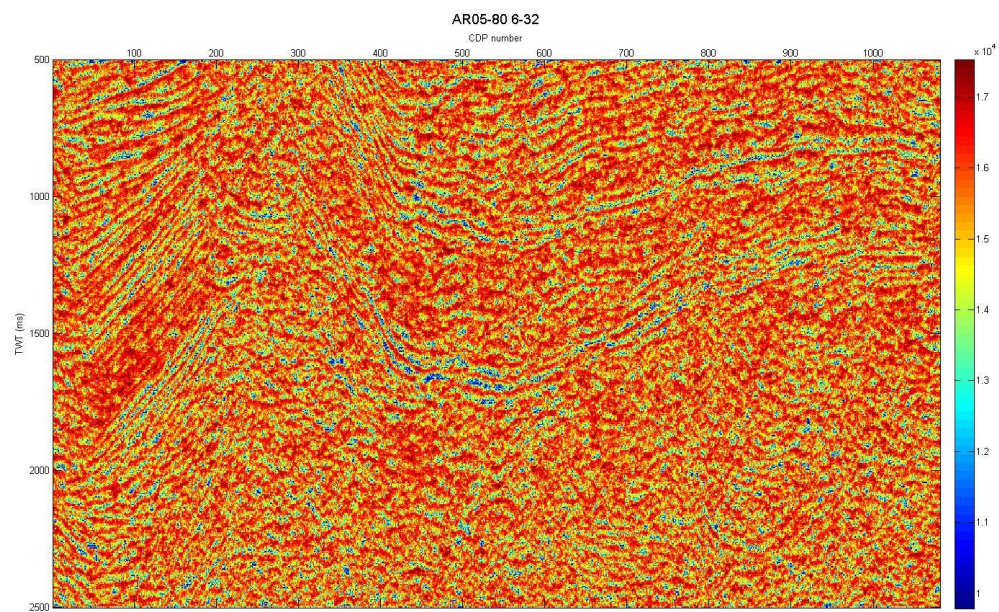


Figure 31 - Result form (6-32) case for the GSI for AR05_80-MIG seismic line.

Presented next are 3 results obtain from a GSI without zones for the **AR09_80-MIG seismic line**. (Figures 32, 33 and 34).

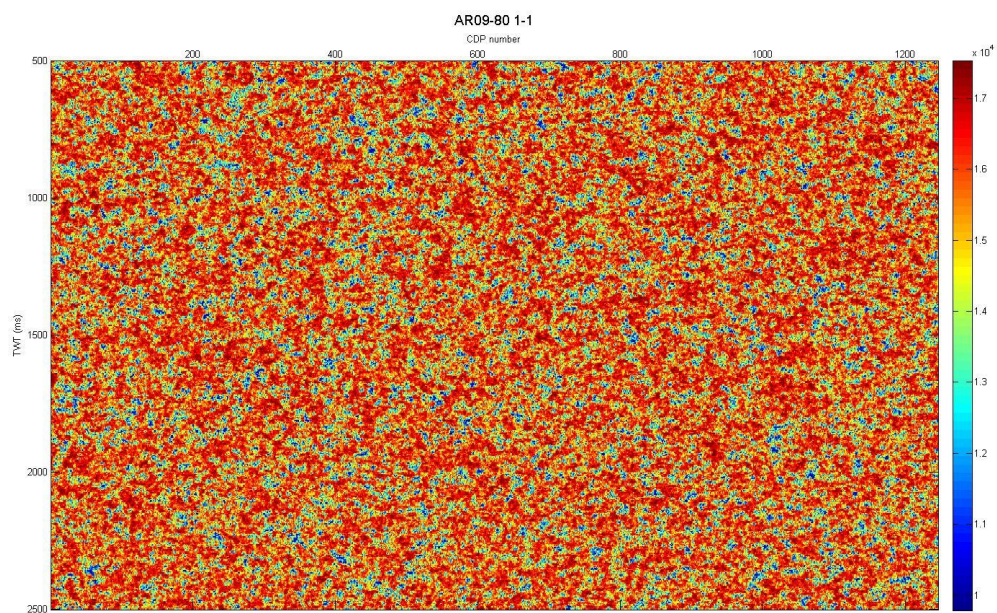


Figure 32 - Result form (1-1) case for the GSI for AR09_80-MIG seismic line

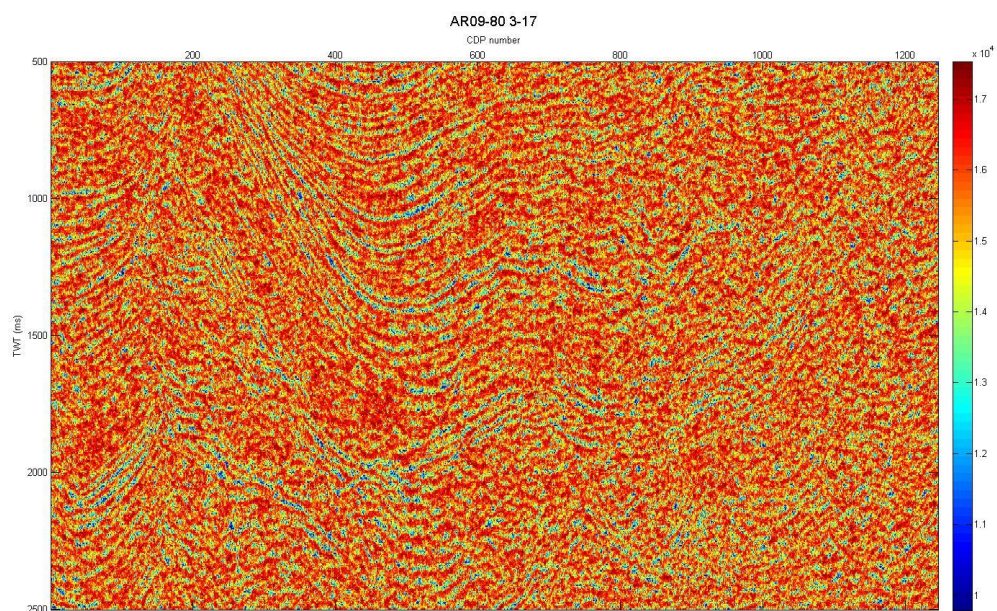


Figure 33 - Result form (3-17) case for the GSI for AR09_80-MIG seismic line.

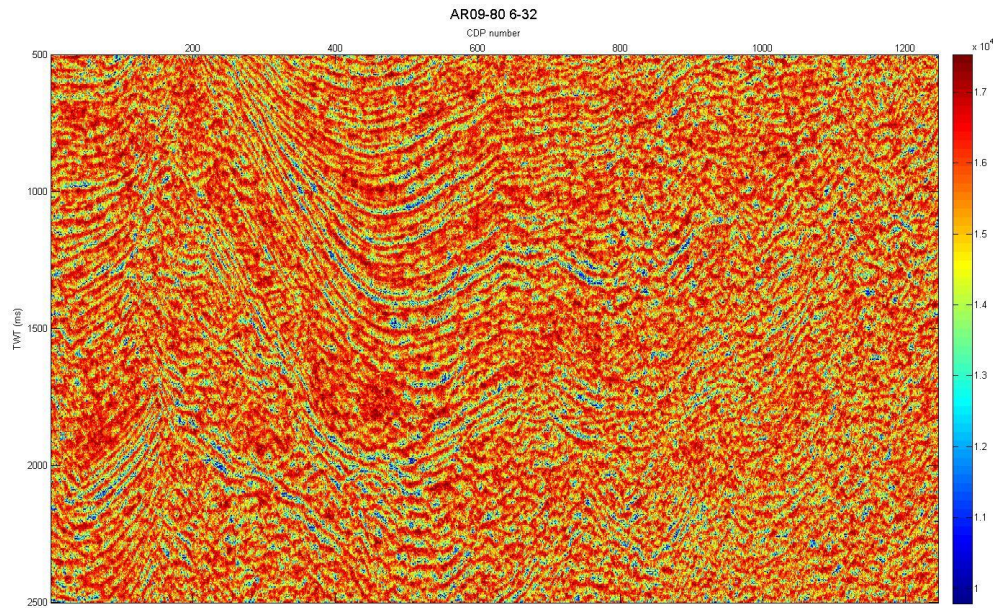


Figure 34 - Result form (6-32) case for the GSI for AR09_80-MIG seismic line.

Generally speaking, the GSI for both seismic lines, AR05_80-MIG and AR09_80-MIG, are good and match with those expected for unexplored areas like this. At the end of the inversion procedure (Figure 31 and 34) the impedance model shows continuous layers that are in concordance with the main seismic reflections.

On figure 29 and 32, correspond realization 1 from the first iteration and therefore the only spatial constrain is the one given by the variogram model used as part of the stochastic sequential simulation. Figures 30 and 31 show the evolution of the inverted model in the middle of the iterative procedure. It is clear that the spatial pattern as interpreted from the seismic data is appearing on the retrieved impedance model.

In terms of correlation coefficient values for both seismic lines the best global correlation coefficient between real and synthetic seismic data is around 0.9, which is a very good value of correlation.

While the convergence of the inversion methodology is good, we may doubt about the distribution of the acoustic impedance values in the retrieved inverse model. There are preferable locations or particular impedance values. Since the impedance values are geological dependent we decided to include the seismic interpretation in the definition of the inversion grid and build acoustic impedance distributions for each zone. Figures 35 and 36 show the delineation of the inversion grid, and its division by zones using the seismic interpretation previously done.

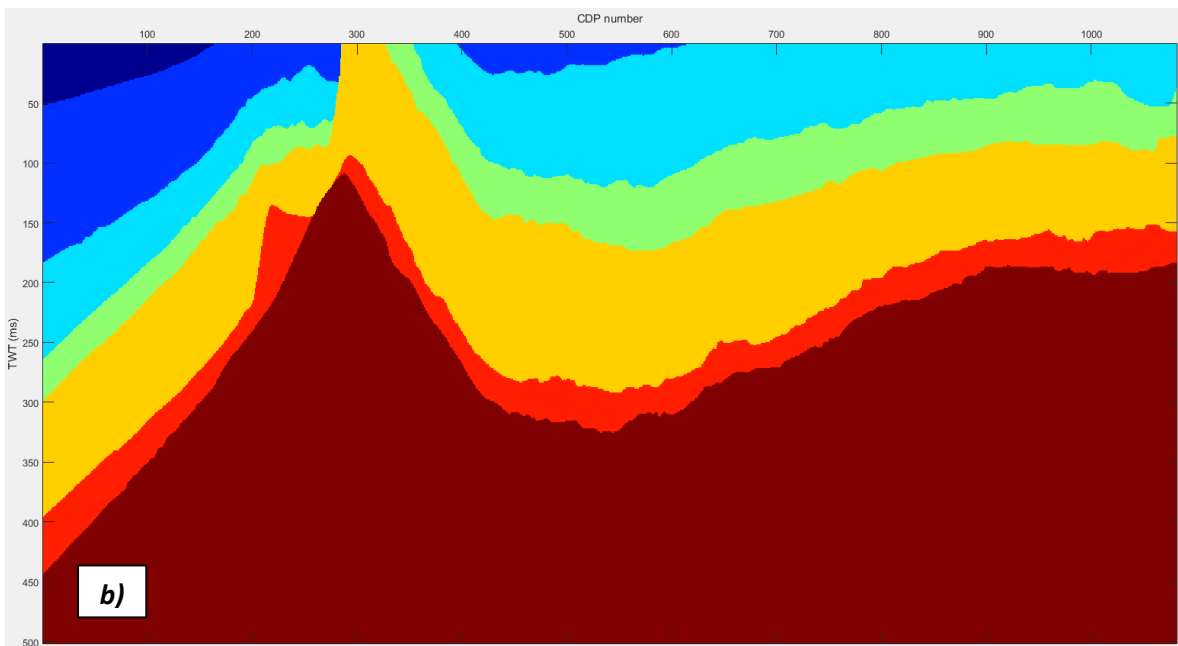
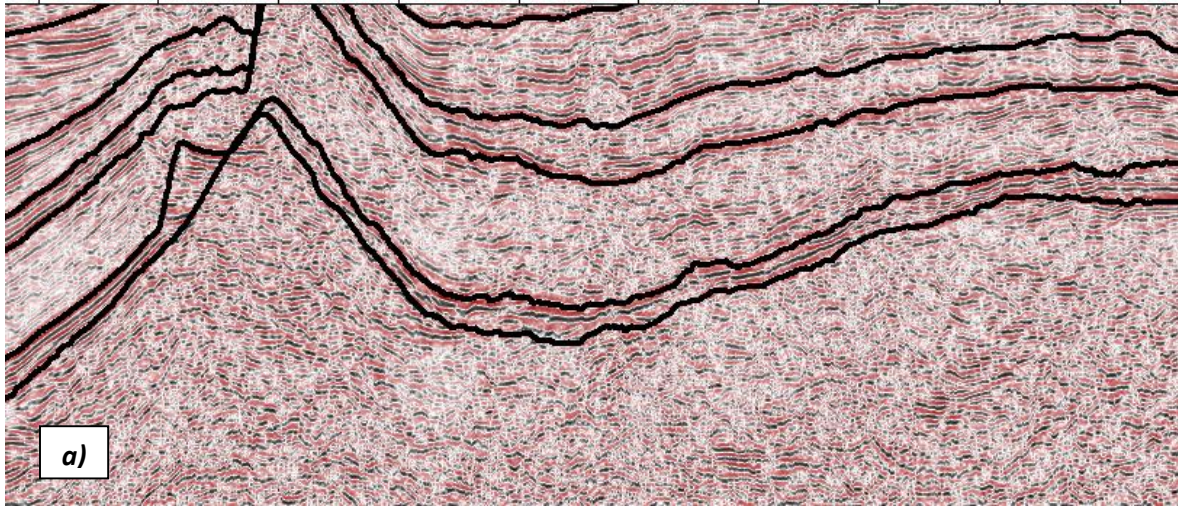


Figure 35 a) and b) - The first image, is the real AR05_80-MIG Seismic line and the horizons marked. The second image is the zones for each of the horizons marked. Note the two images had the seismic already cropped to interest area.

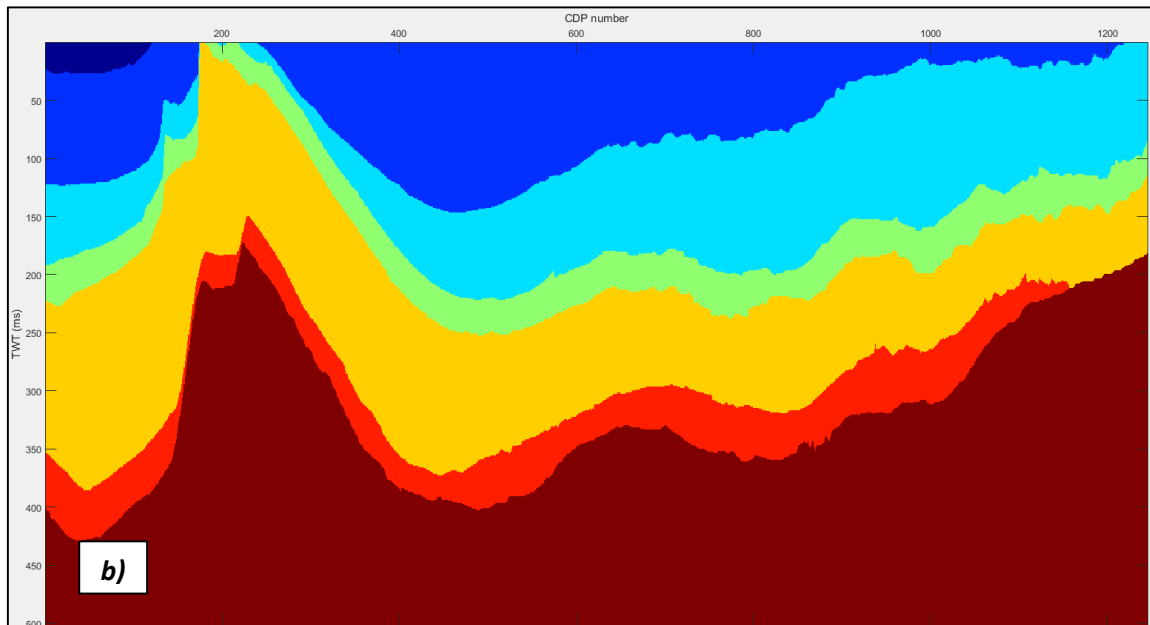
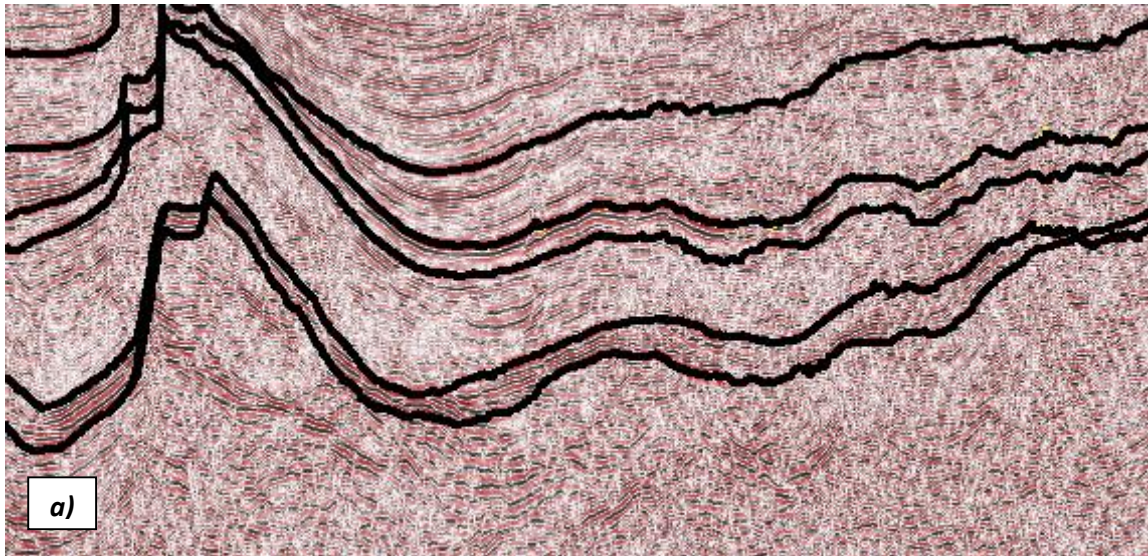


Figure 36 a) and b) - The first image, is the real AR09_80-MIG Seismic Line and the horizons marked. The second image is the zones for each of the horizons marked. Note the two images had the seismic already cropped to interest area.

In terms of conditional distribution for each zone they were retrieved from the Benfeito-1 well and from public data of nearby wells.

The description of the zones on figure 35 and 36:

Zone 0 – Is the interval of the Upper Jurassic Sediments, which are from 0-135m of depth on the Benfeito-1 well report.

Zone 1 – Corresponds to the interval of the Abadia Formation, and to compute the value for AI, because the RHOB log only started at the 995meters of depth in the well, an equation was used to deduce the density from the velocity log, see figure 37.

This equation is Gardner's equation:

$$\rho = d \times V_p^f$$

Equation 1 – Gardner's Equation

This is an empirical equation to be used when the V_p is known but the density not. The d and f coefficients are chosen based on the lithology of the formation, in this case the one applied was for limestone and proposed by Gardner, which are 1.36 for d and 0.38 for f , see equation 6.

Zone 2, Zone 3 & Zone 4 – Corresponds to Montejunto Formation, Cabaços Formation and Brenha (Aalenian-Pliensbachian) Formation respectively were computed using the normally the Velocity Log and RHOB log.

Zone 5 – Corresponds to the Dagorda Formation, in this case the Velocity log and RHOB logs end at the 3273m, which is not corresponding to the end of this formation, so the acoustic impedance was computed using the values that we have, extended to all the thickness formation.

Zone 6 – Corresponds to the Grés de Silves Formation, also considered the Basement on the interpretation, and for this there is no logging information, no RHOB or Velocity. So according to a gravimetric modeling paper (Miranda et al., 2010) the average density for this formation is 2.9 g/cm³ and according to the MILUPOBAS report the velocity is around 5000 to 5500 m/s. AI values were generated randomly based on this mean and variance values.

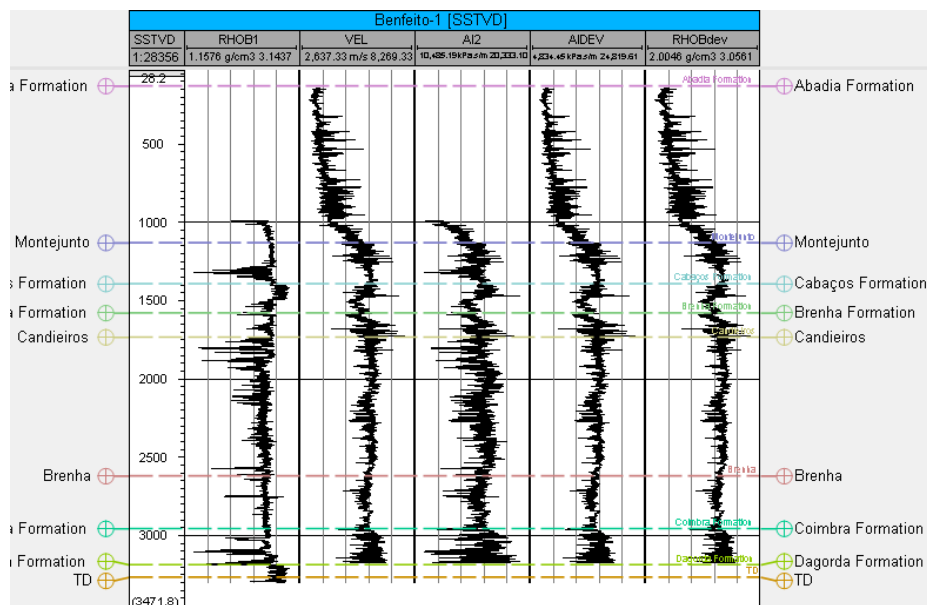


Figure 37 - Log data from the Benfeito well. Track 1 the RHOB log; track 2 the Velocity log; track 3 the AI calculated from track 1 and 2; track 4 the AI resulting from the derivation of the Gardner's equation and last track 5 the RHOB obtain with the Gardner's equation.

For the GSI with zones, the results presented in this work will be the same 3 cases for the (1-1), (3-17) and (6-32) already used to compare the GSI without zones. Presented next are the results for the AR05_80-MIG seismic line using the GSI with zones (Figure 38, 39 and 40), and on figure 41 the corresponding correlations coefficient values.

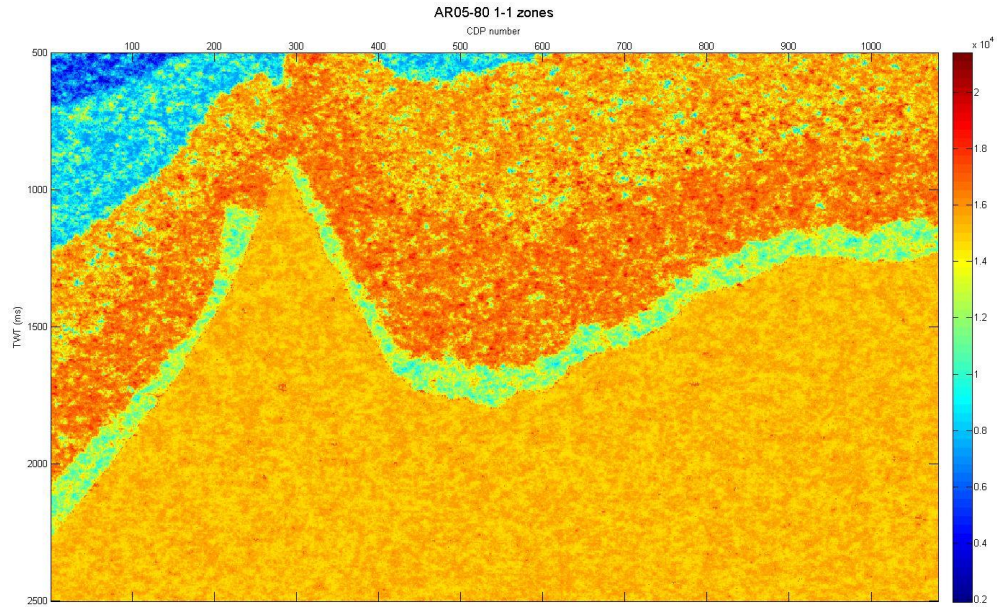


Figure 38 - Result form (1-1) case for the GSI with zones for AR05_80-MIG seismic line

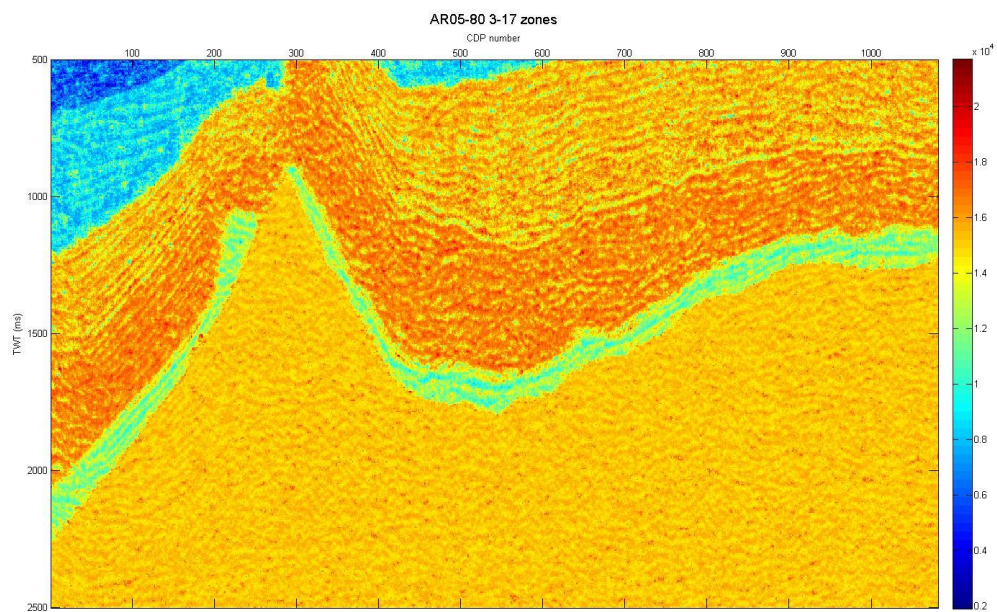


Figure 39 - Result form (3-17) case for the GSI with zones for AR05_80-MIG seismic line

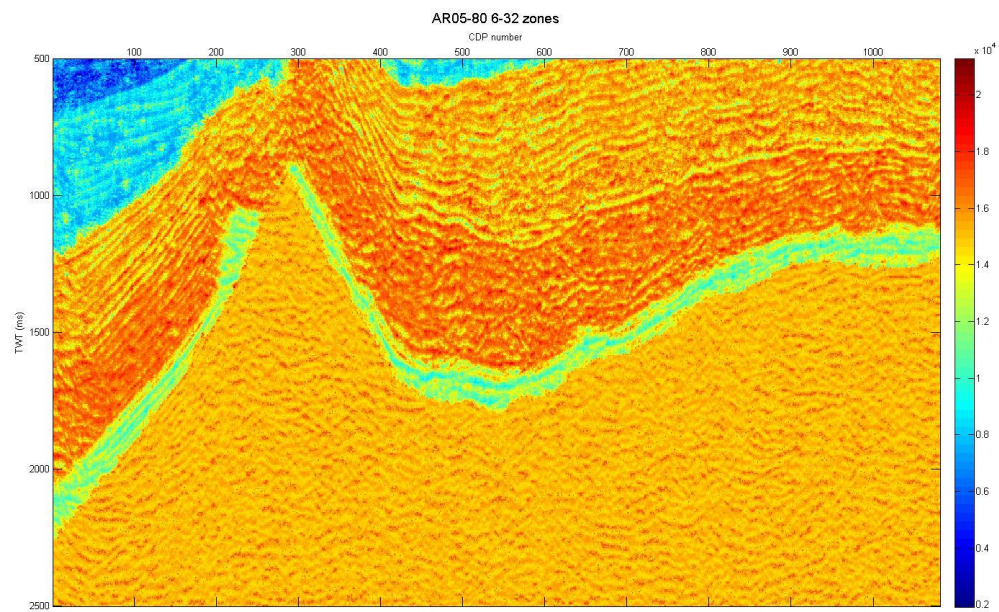


Figure 40 - Result form (6-32) case for the GSI with zones for AR05_80-MIG seismic line

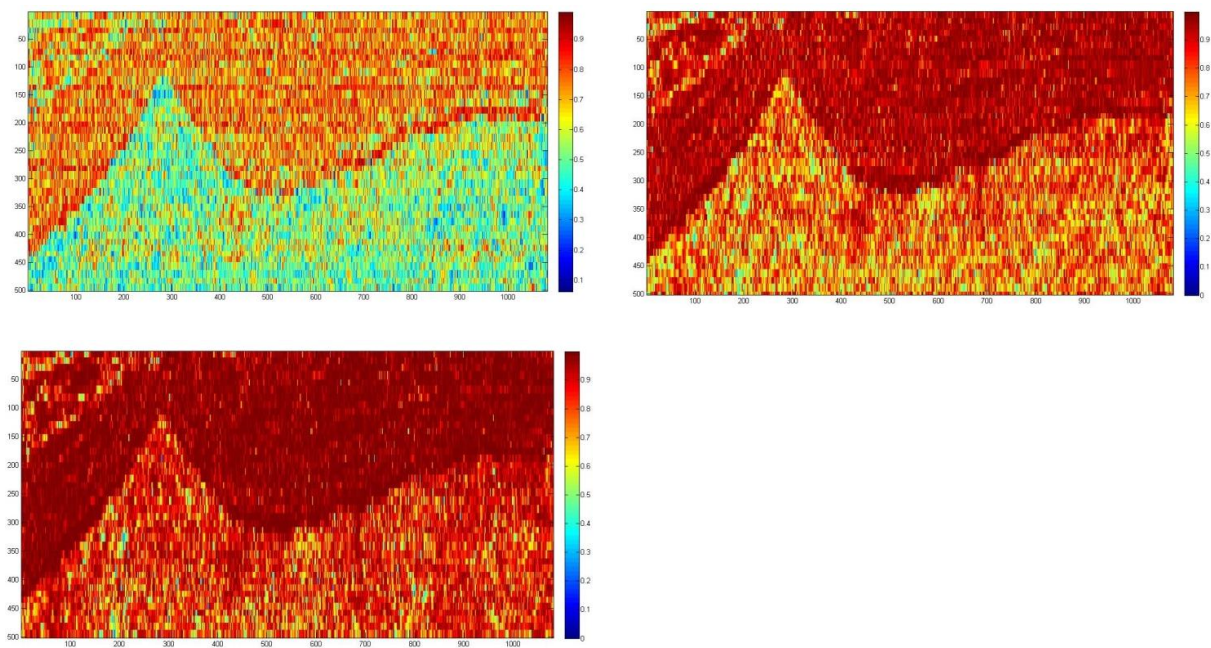


Figure 41 - Correlation Coefficient Values for the corresponding 3 images on figure 38, 39 and 40.

Presented next is the result for the AR059_80-MIG seismic line for the GSI with zones (Figure 42, 43 and 44), and on figure 45 the corresponding correlations coefficient values.

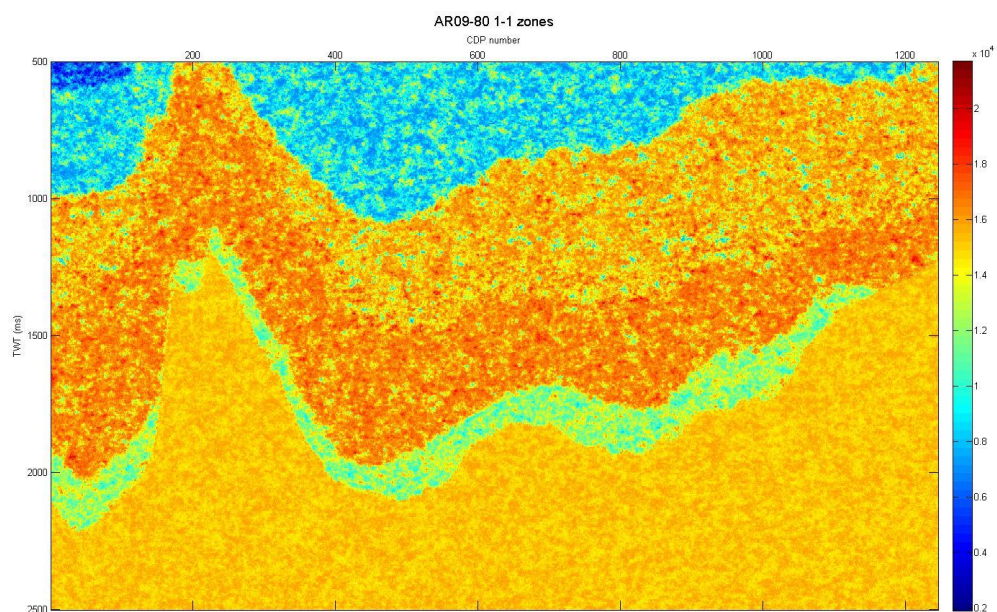


Figure 42 - Result form (1-1) case for the GSI with zones for AR09_80-MIG seismic line

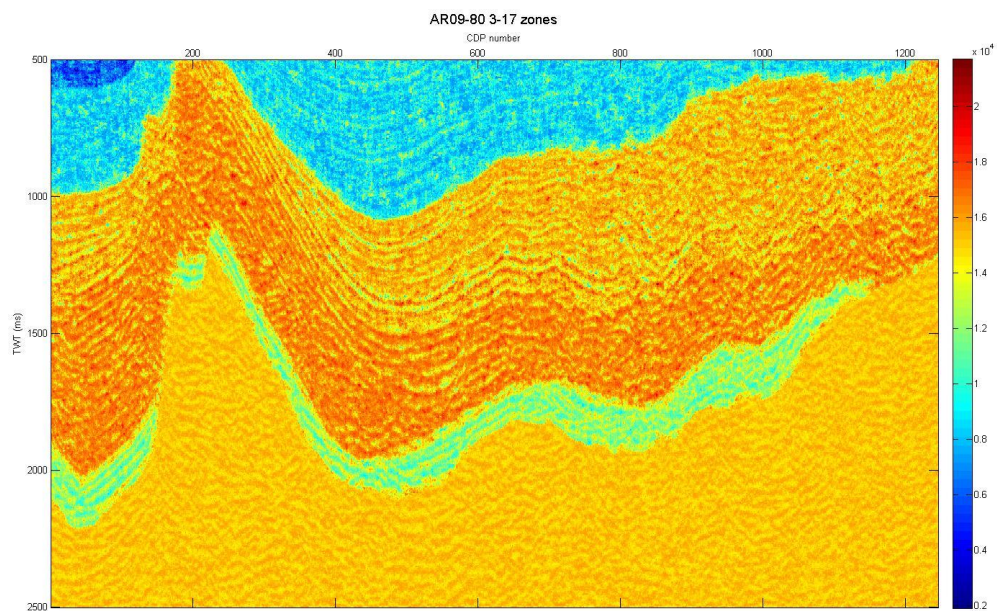


Figure 43 - Result form (3-17) case for the GSI with zones for AR09_80-MIG seismic line

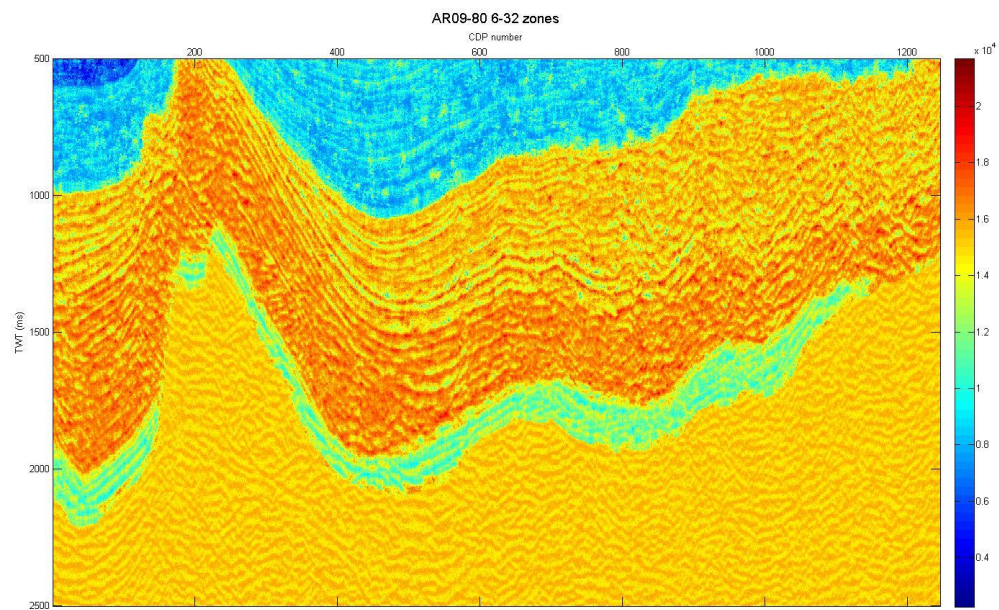


Figure 44 - Result form (6-32) case for the GSI with zones for AR09_80-MIG seismic line

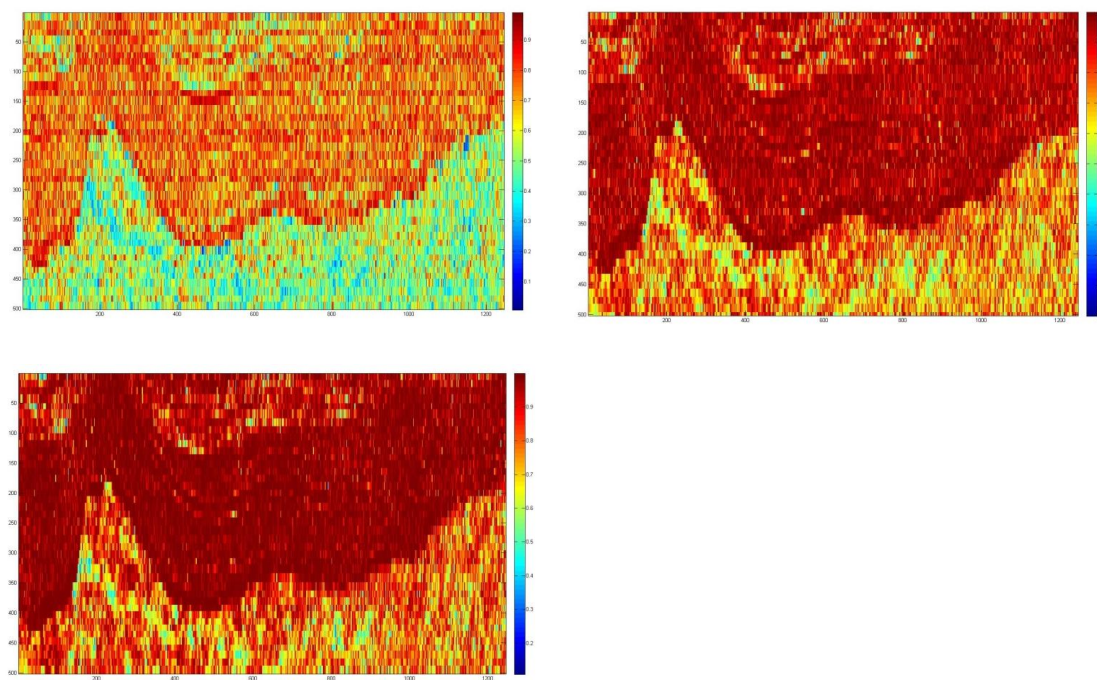


Figure 45 - Correlation Coefficient Values for the corresponding 3 images on figure 42, 43 and 44.

In both seismic lines, AR05_80-MIG and AR09_80-MIG the GSI the retrieved acoustic impedance models seem plausible and do agree with the observed seismic. As expected in the areas where the seismic do not present a good quality and a low signal to noise ratio, the spatial continuity is reduced, and the corresponding coefficient correlation are low at the end of the inversion procedure.

The center zones in both seismic lines (AR05_80 and AR9_80) are the ones that present a better convergence of the model and the best correlation values closest to 1, due to the presence of strong reflectors well replicated on the acoustic impedance GSI images.

In this areas the uncertainty of the model is high, is the case of the last zone (zone 6), the equivalent to Grés de Silves and Basement formation on both seismic lines, the seismic is highly chaotic and the values in terms of correlation still very low. Remember that the values used for the hard data in this zone were calculated regarding data from density and velocity of some authors, which bring even more uncertainty.

In terms of convergence of the application of the GSI, the results between the real seismic and the synthetic in both of the Seismic lines were good, and the main reflectors are well reproduced (Figure 46 and 47).

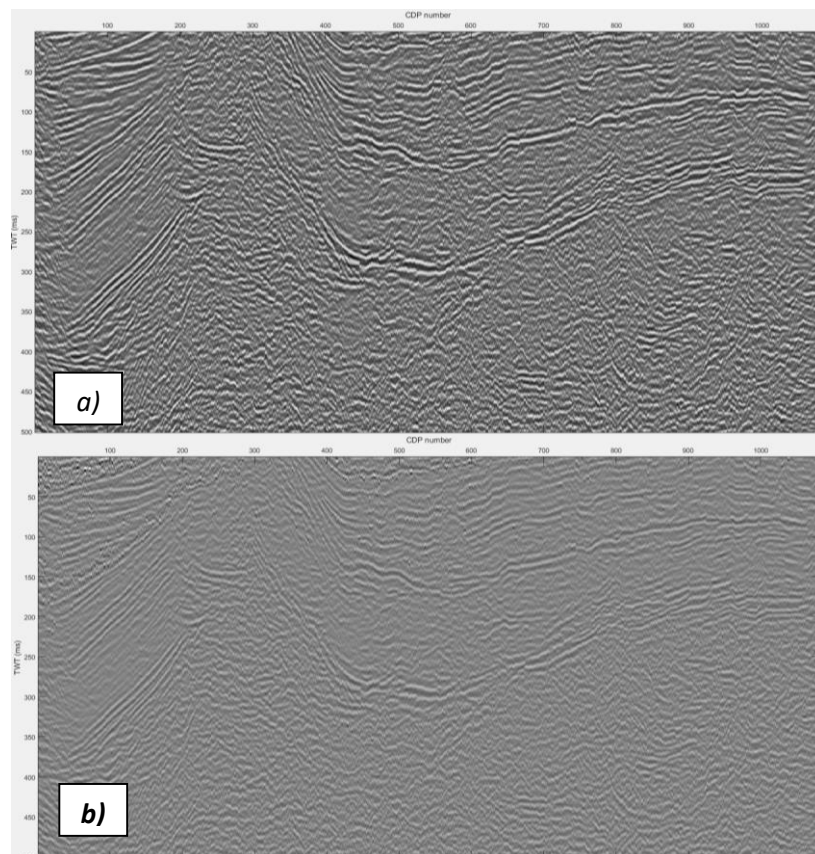


Figure 46 a) and b) - Seismic lines AR05_80-MIG, a) - real and b) - synthetic seismic.

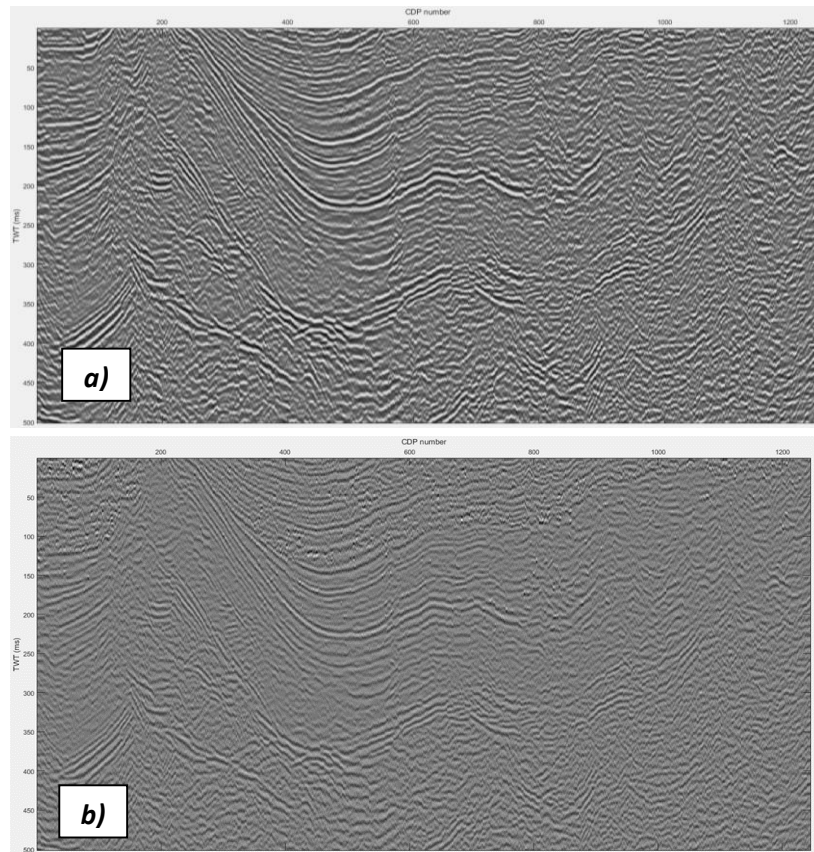


Figure 47 a) and b) - Seismic lines AR05_80-MIG, a) - real and b) - synthetic seismic.

5.5 Integration of the Interpretation

This work was successfully done, in terms of the different types of information, available and studied for the Arruda Sub-basin, Portugal.

In terms of Geological Framework, the regional geology information was summarized, for the Lusitanian basin and for the geodynamics and tectonics of the Arruda Sub-basin.

For the well logging data, Petrophysical values were calculated successfully, for the different stratigraphic units on the Benfeito-1 well. The results obtained are not very encouraging in terms of hydrocarbon accumulations, but provide a better analysis of the lithology in each layer.

On the Seismic Interpretation chapter, the two 2D seismic lines, were re-interpreted according to structural and stratigraphic analyses and with the known well tops, corresponding to Benfeito-1 well.

And last for the Geostatistical Seismic Inversion (GSI), with and without zones, the process was new, for this kind of under-explored areas. The results were encouraging in terms of the characterization of the sub-surface elastic properties, but more data needs to be added, to get better and more accurate results.

6. Conclusion

This study shows the importance of data integration particularly for unexplored sedimentary basins as the Arruda sub-basin. We integrated all the available information in terms of geology, petrophysics and geostatistical modeling to characterize the spatial distribution of the subsurface properties of interest, i.e. acoustic impedance.

For this part of the Arruda Sub-basin, with the analysis of the real data, we can infer that is a very promising area in terms of possible hydrocarbon accumulations, based not only on the petrophysical interpretation but also on the inverted models that show consistent low acoustic impedance values for layers at the same depth.

This work should now be improved with the integration of other nearby wells and seismic reflection lines improving in this way the petrophysical and seismic interpretations, which will allow more reliable acoustic impedance models.

The results presented here an added value for the knowledge of this sub-basin. At our knowledge this is the first time a subsurface elastic model is presented for this area. Also, this work presents a reliable solution for the application of geostatistical seismic inversion methodologies where only few well data is available.

7. References

- Alves, T.M., Manuppella, G., Gawthorpe, R.L., Hunt, D.W. & Monteiro, J.H. (2003) – *The depositional evolution of diapir-and fault-bounded rift basins: examples from the Lusitanian Basin of West Iberia*. Sedimentary Geology.
- Alves, T. M. et al (2009) - *Diachronous evolution of Late Jurassic–Cretaceous continental rifting in the northeast Atlantic (west Iberian margin)* Tectonics Volume 28.
- Asquith G., Krygowski D. (2006), - *Basic Well Log Analysis, Second Edition*, AAPG Methods in Exploration Series, No. 16.
- Azevedo, L. (2013) - *Geostatistical methods for integrating seismic reflection data into subsurface Earth models*. Lisboa: Instituto Superior Técnico.
- Bosch, Miguel, Tapan Mukerji, and Ezequiel F. González. (2010). *Seismic Inversion for Reservoir Properties Combining Statistical Rock Physics and Geostatistics: A Review*. Geophysics 75.
- Azevedo L. (2009). - *Seismic Attributes in Hydrocarbon Reservoirs Characterization*. Universidade de Aveiro, Master thesis in Geological Engineering
- Caetano, H. (2009). - *Integration of Seismic Information in Reservoir Models: Global Stochastic Inversion*. Lisboa: Instituto Superior Técnico.
- Ellis, P.M., Wilson, R.C.L., Leinfelder, R.R., 1990. *Controls on Upper Jurassic carbonate buildup development in the Lusitanian Basin, Portugal*. Spec. Publ. Int. Assoc. Sedimentol. 9.
- E. M Gradstein, M.G. Willis, R.C.L Wilson, R. N. Hiscott (1989) *The Lusitanian Basin of west central Portugal: Mesozoic and Tertiary tectonics, stratigraphy and subsidence history*. In: Extensional Tectonics and Stratigraphy of the North Atlantic Margins. Am. Assoc. Pet. Geol. Mem.
- Filippova, K., A. Kozhenkov, and A. Alabushin. (2011). *Seismic Inversion Techniques: Choice and Benefits*. First Break 29 (May).
- Francis, AM. (2006). *Understanding Stochastic Inversion: Part 1*. First Break 24 (November).
- GPEP, (1983) – *Benfeito-1, Relatório final de Sondagem*.
- J. Carvalho et al, (2005) - *The structural and sedimentary evolution of the Arruda and Lower Tagus sub-basins, Portugal*. Marine and Petroleum Geology 22.
- J. C. Kullberg, R. B. Rocha, A. F. Soares, J. Rey, P. Terrinha, A. C. Azerêdo, P. Callapez, L. V. Duarte, M. C. Kullberg, L. Martins, R. Miranda, C. Alves, J. Mata, J. Madeira, O. Mateus, M. Moreira C. R. Nogueira (2013) *A Bacia Lusitaniana: Estratigrafia, Paleogeografia e Tectónica, -Geologia de Portugal*, Volume 2, Escolar Editora

Kullberg, J.C.R. (2000) – *Evolução tectónica Mesozóica da Bacia Lusitaniana*. Tese Doutoramento (n. publ.), Universidade Nova de Lisboa, Portugal.

Leinfelder, R.R., Wilson, R.C.L., 1989. *Seismic and sedimentologic features of the Oxfordian–Kimmeridgian syn-rift sediments on the eastern margin of the Lusitanian Basin*. Geol. Rundsch. 78.

Lomholt, S., Rasmussen, E.S., Andersen, C., Vejbaek, O.V., Madsen, L., Steinhardt, H., 1996. *Seismic interpretation and mapping of the Lusitanian Basin, Portugal. Contribution to the MILUPOBAS project*, EC Contract No. J0U2-CT94-0348, Geological Survey of Denmark.

Mavko, Gary, Tapan Mukerji, and Jack Dvorkin. (2003) -*The Rock Physics Handbook*. Cambridge University Press.

Miranda, J. P. (2009) - *Aquisição e modelação de dados gravimétricos sobre o diapíro salino de Matacães, Torres Vedras, Bacia Lusitânica*. Dissertação (Mestrado) – Universidade de Coimbra, Departamento de Ciências da Terra, Portugal

Pena R, Pimentel N, (2014) - *Analysis of the Petroleum Systems of the Lusitanian Basin (Western Iberian Margin) — A Tool for Deep Offshore Exploration, Sedimentary Basins, Origin, Depositional Histories, and Petroleum Systems*.

P, Gonçalves (2015) -*Palynofacies and source rock potential of Jurassic sequences on the Arruda sub-basin (Lusitanian Basin, Portugal)*. Marine and Petroleum Geology 59.

Rasmussen, E.S., Lomholt, S., Andersen, C. & Vejbaek, O.V. (1998) – *Aspects of the structural evolution of the Lusitanian Basin in Portugal and the shelf and slope area offshore Portugal*. Tectonophysics,

Ravnås, R., Windelstad, J., Mellere, D., Nøttvedt, A., Stühr Sjøblom, T., Steel, R.J., Wilson, R.C.L., 1997. *A marine Late Jurassic synrift succession in the Lusitanian Basin, Western Portugal — Tectonic significance of stratigraphic signature*. Sediment. Geol. 114

Soares, A. (2001) – *Direct sequential simulation and cosimulation*. Mathematical Geology, 33(8).

Soares, Amílcar, JD Diet, and Luis Guerreiro. (2007) - *Stochastic Inversion with a Global Perturbation Method*. Petroleum Geostatistics, EAGE, Cascais, Portugal (September 2007).

Wilson, R. C. L. (1979) - *A reconnaissance study of Upper Jurassic sediments of the Lusitanian Basin*. Ciências da Terra, Univ. Nov. Lisboa.

Wilson, R. C. L. (1988) – *Mesozoic development of the Lusitanian Basin, Portugal*. Rev. Soc. Geol. España, I.

Yilmaz, O. (2001) - *Seismic data analysis: processing, inversion, and interpretation of seismic data*. SEG, Tulsa (OK), 1 vol.

Zbyszewski, G. (1964) - Carta Geológica dos Arredores de Lisboa na Escala 1/50 000 e Notícia Explicativa da Folha 34-B LOURES. Serviços Geológicos de Portugal. Lisboa.

Zbyszewski, G.; Torre de Assunção, C. (1965) - Carta Geológica de Portugal na Escala 1/50 000 e Notícia Explicativa da Folha 30-D ALENQUER. Serviços Geológicos de Portugal. Lisboa.

Zbyszewski, G.; Veiga Ferreira, O.; Manuppella, G., Torre Assunção, C. (1966) - Carta Geológica de Portugal na Escala 1/50 000 e Notícia Explicativa da Folha 30-B BOMBARRAL. Serviços Geológicos de Portugal. Lisboa.